Chemistry–A European Journal

Supporting Information

Inducing Curvature to Pyracylene upon π-Expansion

John Bergner, Christian Walla, Frank Rominger, Andreas Dreuw, and Milan Kivala*

Table of contents

1. General Experimental Methods

1.1. General Reaction Conditions

All solvents and reagents were purchased at reagent grade from commercial suppliers (Merck/Sigma-Aldrich, TCI, Thermo Fisher Scientific, Acros Organics, Honeywell) and used without additional purification. All reactions were performed in sealed Biotage microwave reaction vials (10–20 mL, or 2.0–5.0 mL in combination with aluminum caps and septa). Thin layer chromatography was monitored on ALUGRAM aluminum plates from Macherey-Nagel, coated with 0.20 mm SiO_2, by irradiation with UV-light (λ= 365 and 254 nm). Flash column chromatography was carried out with SiO_2 from Macherey-Nagel (technical grade 60 M, pore size 60 Å, 40−63 µm particle size).

1.2. Instruments Used

Nuclear Magnetic Resonance spectra were recorded at room temperature (295 K) on a Bruker Avance III 300, 400, 500, 600 or 700 at the Institute of Organic Chemistry (University of Heidelberg). Proton broad band decoupling was applied for ^{13}C measurements. Deuterated solvents were used as purchased from Merck/Sigma-Aldrich. Chemical shifts (reported in parts per million ppm) were referenced[1] to δ_H = 7.26 ppm ($CDCl_3$) and 5.32 ppm (CD_2Cl_2) for ^1H and δ_C = 77.16 ppm ($CDCl_3$) and 53.84 ppm (CD_2Cl_2) for ^{13}C and interpreted with MestReNova Version 14.1.2-25024. Multiplicity is reported as s (singlet), d (doublet), dd (doublet of doublets), t (triplet), or m (multiplet).

UV-Vis Absorption and Emission Spectra. UV-Vis spectra were recorded on an Agilent Cary 60 UV-Vis spectrometer and measured in CH_2Cl_2 in the wavelength region of 230 to 800 nm under ambient conditions (room temperature (rt)). The abbreviations br (broad) and sh (shoulder) refer to saddle points or shoulders in the absorption spectrum. Fluorescence spectra were recorded on a JASCO FP-8500 Fluorescence Spectrometer. The photoluminescence quantum yields (PLQYs) were estimated with a JASCO ILF-835 (100 mm) integrating sphere. The data were processed by using Spectra Manager from JASCO.

X-ray Crystallography. Single crystals were obtained by slow gas phase diffusion of MeOH into a solution of the compounds in toluene or 1,2-dichlorobenzene at rt. The Bruker APEX-II Quazar diffractometer (radiation MoKα, λ = 0.71073 Å) with a CCD area detector and the STOE Stadivari instrument (radiation CuKα, λ=1.54178 Å) with a Pilatus CCD area detector (0.5° ω-scans) were used for data collection by the X-ray crystallography facility of the Institute of Organic Chemistry (University of Heidelberg). Structures were solved with the ShelXT[2] structure solution program and refined against F^2 with a full-matrix least-squares algorithm with ShelXL.[3] Hydrogen atoms were treated with riding models. Graphical visualization and analysis of the structural parameters was carried out with Mercury 2020.1.[4]

Cyclic Voltammetry. A BASi Cell Stand instrument with a glassy carbon disk working electrode (3.0 mm diameter), an Ag/AgCl (3M NaCl) quasi-reference electrode, and a platinum wire auxiliary electrode were used to record cyclic voltammograms. Before each measurement, a 0.1 M electrolyte solution of *n*-Bu_4NPF_6 in anhydrous CH_2Cl_2 was degassed with nitrogen for 20 min. The respective compounds were measured at a scan rate of 149 mV s^{-1}, followed by the addition of ferrocene as the internal standard and re-measurement.

Infrared Spectroscopy. Infrared spectra were recorded on a JASCO FT/IR-6000 FTIR spectrometer operated in an ATR mode at ambient conditions. The obtained transmission spectra are baseline corrected, plotted in cm^{-1} and labeled according to the following abbreviations: s (strong), m (medium), w (weak), and br (broad).

Melting Point. The melting point was determined on a Büchi M-560 melting point apparatus in open capillaries. Decomp. refers to decomposition.

Mass Spectrometry. Mass spectra were recorded at the facility of the Institute of Organic Chemistry (University of Heidelberg) and recorded on a JEOL AccuTOF GCx (electron ionization (EI)) or a Bruker timsTOFfleX (matrix assisted laser desorption ionization (MALDI)) instrument.

Theoretical calculations. The DFT calculations were carried at the B3LYP-D/6-31G(d) and CAM-B3LYP/6-31G(d) level of theory using Gaussian16[5] and Q-Chem 5.4.[6] NICS(–1/0/+1) values were determined adopting the B3LYP functional together with the 6-31G(d) Gaussian basis set and precisely positioned dummy atoms. Frequency calculations were carried out to characterize the optimized structures as ground state equilibrium structures. Excited-state calculations were performed within the linear response time-dependent (TD) DFT[7] approximation using the polarizable continuum model for solvation (ε (CH_2Cl_2) = 8.93).

2. Synthesis

Compounds **S1**, **S2**, **S3**, and **S4** were synthesized according to modified literature procedures.

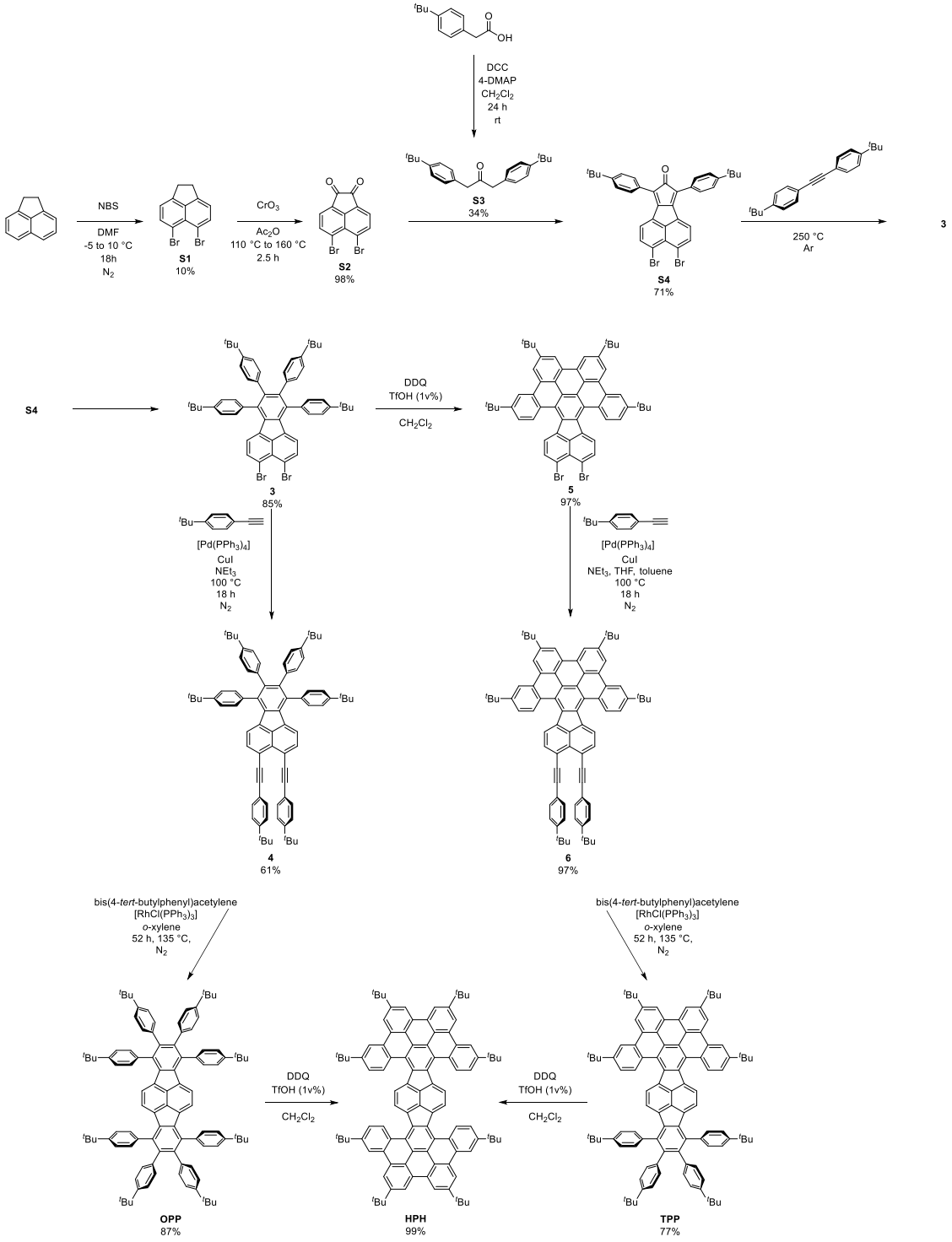

Figure S1: Synthetic route towards compounds **OPP**, **TPP** and **HPH**. DMF = *N*,*N*-dimethylformamide, NBS = *N*-bromosuccinimide, DCC = *N*,*N*'-dicyclohexylcarbodiimide, 4-DMAP = 4-(dimethylamino)pyridine, DDQ = 2,3-dichloro-5,6-dicyano-1,4-benzoquinone, TfOH = triflic acid, THF = tetrahydrofuran.

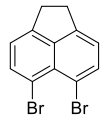

$C_{12}H_8Br_2$
312.00 g/mol

5,6-Dibromo-1,2-dihydroacenaphthylene (S1).[8]

A stirred suspension of acenaphthene (40.0 g, 259 mmol) in dry DMF (250 mL) was cooled to 0 °C. Over the course of 3 h there was added NBS (115 g, 648 mmol) in portions. After additional 2 h of stirring the temperature was raised to 10 °C and the suspension stirred overnight. The cooled mixture was filtered to give a crude colorless product which was purified by recrystallization from $CHCl_3$ and MeOH mixture. Compound **S1** (8.39 g, 26.9 mmol, 10%) was obtained as colorless crystals.

M.p.: 174–175 °C (lit. 174–176).[8]

R_f = 0.60 (SiO_2, PE).

^{1}H NMR (400 MHz, $CDCl_3$): δ = 7.80 (d, *J* = 7.4 Hz, 2H), 7.10 (d, *J* = 7.5 Hz, 2H), 3.31 (s, 4H) ppm.

^{13}C NMR (100 MHz, $CDCl_3$): δ = 147.2, 142.2, 136.0, 128.0, 121.1, 114.6, 30.2 ppm.

IR (FT-ATR): $\tilde{\nu}$ = 2945 (w), 1857 (w), 1597 (m), 1408 (m), 1321 (m), 1224 (m), 1105 (m), 1020 (m), 833 (s), 705 (m), 600 (s) cm^{-1}.

HRMS (EI): calcd. for $C_{12}H_8{}^{79}Br_2$: 309.89873 [M^+]; found: 309.89846.

The characterization data are in agreement with those reported.

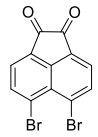

$C_{12}H_4Br_2O_2$
339.97 g/mol

5,6-Dibromoacenaphthylene-1,2-dione (S2).[9]

A 20 mL reaction tube was charged with **S1** (50.0 mg, 160 µmol) and Ac_2O (5.00 mL). The tube was warmed to 110 °C until the starting material was fully dissolved. Chromium(VI) oxide (160 mg, 1.60 mmol) was added in portions over a time period of 30 min and the reaction mixture was heated to 160 °C for 1.5 h. The boiling reaction mixture was filtered through a pad of hot sand and the filtrate was cooled to 7 °C. After filtration compound **S2** (53.2 mg, 156 µmol, 98%) was afforded as an orange solid.

M.p.: 326–328 °C (lit. 326–328).[10]

R_f = 0.24 (SiO_2, PE/EtOAc 6:1).

^{1}H NMR (301 MHz, $CDCl_3$): δ = 8.26 (d, *J* = 7.6 Hz, 2H), 7.93 (d, *J* = 7.6 Hz, 2H) ppm.

^{13}C NMR: Insolubility of the compound in common deuterated solvents prevented to obtain a meaningful spectrum.

IR (FT-ATR): $\tilde{\nu}$ = 3443 (w), 3072 (w), 3048 (w), 1912 (w), 1767 (w), 1724 (s), 1609 (m), 1590 (m), 1549 (s), 1468 (m), 1408 (m), 1351 (m), 1309 (m), 1268 (m), 1220 (m), 1200 (m), 1151 (m), 1108 (m), 1024 (s), 908 (m), 840 (s), 796 (m), 757 (m), 726 (s) cm^{-1}.

HRMS (LDI): calcd. for $C_{12}H_5{}^{79}Br_2O_2$: 338.8651 [M+H$^+$]; found: 338.8641.

The characterization data are in agreement with those reported.

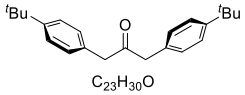

$C_{23}H_{30}O$
322.49 g/mol

1,3-Bis(4-*tert*-butylphenyl)propan-2-one (S3).[11]

A 250 mL reaction flask was charged with 4-DMAP (953 mg, 7.80 mmol), DCC (5.90 g, 28.6 mmol) and CH_2Cl_2 (50.0 mL). Subsequently (4-*tert*-butylphenyl)acetic acid (5.00 g, 26.0 mmol) dissolved in CH_2Cl_2 (50.0 mL) was added dropwise over a time period of 20 min. The reaction mixture was stirred for 24 h at rt. The formed precipitate was filtered off and the crude product obtained after evaporation of the solvent was subjected to column chromatography (SiO_2, PE/EtOAc 10:1). Compound **S3** (2.86 g, 8.86 mmol, 34%) was obtained as a yellow solid.

M.p.: 84 °C.

R_f = 0.85 (SiO_2, PE/EtOAc 8:1).

^{1}H NMR (400 MHz, $CDCl_3$): δ = 7.33 (dt, *J* = 8.4, 1.9 Hz, 4H), 7.09 (dt, *J* = 8.3, 1.9 Hz, 4H), 3.69 (s, 4H), 1.31 (s, 18H) ppm.

^{13}C NMR (101 MHz, $CDCl_3$): δ = 206.3, 150.0, 131.2, 129.3, 125.8, 48.7, 34.6, 31.5 ppm.

IR (FT-ATR): $\tilde{\nu}$ = 3092 (w), 3057 (w), 3033 (w), 2954 (s), 2934 (m), 2905 (m), 2864 (m), 2116 (m), 1700 (m), 1666 (m), 1509 (m), 1468 (m), 1434 (m), 1415 (m), 1389 (m), 1362 (m), 1329 (m), 1289 (m), 1263 (m), 1228 (m), 1193 (m), 1165 (m), 1110 (m), 1070 (m), 1020 (m), 967 (m), 921 (m), 893 (m), 836 (m), 816 (s), 781 (m), 759 (m), 711 (m) cm^{-1}.

HRMS (EI): calcd. for $C_{23}H_{30}O$: 322.22912 [M^+]; found: 322.22819.

The characterization data are in agreement with those reported.

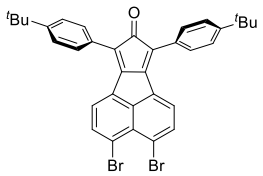

$C_{35}H_{30}Br_2O$
626.43 g/mol

3,4-Dibromo-7,9-bis(4-*tert*-butylphenyl)-8*H*-cyclopenta[*a*]acenaphthylen-8-one (S4).

A microwave tube was charged with **S2** (100 mg, 294 µmol), **S3** (104 mg, 324 µmol) and EtOH (4 mL). The reaction mixture was sonicated to obtain a fine suspension and heated to 90 °C. Then KOH (33.0 mg, 588 µmol) dissolved in EtOH (1 mL) was added dropwise to the hot reaction mixture under continuous stirring. The reaction mixture was heated for additional 20 min and then cooled to rt. Filtration of the crude reaction mixture obtained **S4** (130 mg, 208 µmol, 71%) as a brownish solid.

M.p.: 271 °C (decomp.).

R_f = 0.61 (SiO_2, PE/CH_2Cl_2 3:1).

^{1}H NMR (500 MHz, $CDCl_3$): δ = 7.94 (d, *J* = 7.8 Hz, 2H), 7.86 (d, *J* = 7.8 Hz, 2H), 7.70 (dt, *J* = 8.4, 1.9 Hz, 4H), 7.54 (dt, *J* = 8.4, 2.0 Hz, 4H), 1.39 (s, 18H) ppm.

^{13}C NMR (126 MHz, $CDCl_3$): δ = 201.9, 152.0, 151.7, 146.6, 136.9, 132.6, 129.1, 128.9, 128.2, 125.9, 122.4, 121.6, 120.7, 35.0, 31.4 ppm.

IR (FT-ATR): $\tilde{\nu}$ = 3079 (w), 3039 (w), 2954 (m), 2901 (m), 2864 (m), 1702 (s), 1680 (m), 1604 (m), 1544 (m), 1504 (m), 1463 (m), 1390 (m), 1360 (m), 1320 (s), 1294 (m), 1268 (m), 1224 (m), 1198 (m), 1138 (s), 1108 (m), 1086 (m), 1046 (m), 1011 (m), 958 (m), 930 (m), 836 (s), 824 (s), 792 (m), 713 (m) cm^{-1}.

UV/Vis: (CH_2Cl_2) λ_{max} (ε) 263 (37200) 273 (36400) 358 (18000) 420 (11900) nm (M^{-1} cm^{-1}).

HRMS (MALDI, dctb): calcd. for $C_{35}H_{30}{}^{79}Br_2O$: 624.0658 [M^+]; found: 624.0666.

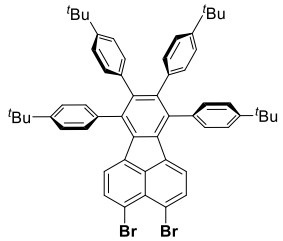

$C_{56}H_{56}Br_2$
888.87 g/mol

3,4-Dibromo-7,8,9,10-tetrakis(4-*tert*-butylphenyl)fluoranthene (3).

A microwave tube was charged with **S4** (50.0 mg, 79.8 µmol) and bis(4-*tert*-butylphenyl)acetylene (23.2 mg, 79.8 µmol) under argon atmosphere. The sealed tube was maintained at 250 °C for 18 h. After cooling to rt, the crude material was subjected to column chromatography (SiO_2, PE/CH_2Cl_2 10:1) to afford the desired compound **3** (58.3 mg, 65.6 µmol, 85%) as a yellow crystalline solid.

M.p.: 333–335 °C.

R_f = 0.86 (SiO_2, PE/CH_2Cl_2 3:1).

^{1}H NMR (400 MHz, CD_2Cl_2): δ = 7.41 (d, *J* = 7.7 Hz, 2H), 7.11 (d, *J* = 8.3 Hz, 4H), 6.94 (d, *J* = 8.2 Hz, 4H), 6.67 (d, *J* = 8.3 Hz, 4H), 6.57 (d, *J* = 8.3 Hz, 4H), 6.05 (d, *J* = 7.7 Hz, 2H), 1.10 (s, 18H), 0.88 (s, 18H) ppm.

^{13}C NMR (101 MHz, CD_2Cl_2): δ = 150.7, 148.7, 142.3, 138.1, 137.8, 137.4, 136.9, 136.4, 136.2, 135.5, 131.3, 129.8, 126.9, 125.5, 124.5, 123.8, 119.6, 34.9, 34.4, 31.5, 31.3 ppm.

IR (FT-ATR): $\tilde{\nu}$ = 3084 (w), 3061 (w), 3033 (w), 2952 (m), 2901 (w), 2864 (w), 1901 (w), 1669 (w), 1609 (w), 1561 (w), 1513 (m), 1461 (m), 1404 (m), 1360 (m), 1268 (m), 1222 (m), 1201 (m), 1173 (m), 1119 (m), 1064 (m), 1020 (m), 965 (m), 948 (m), 831 (m), 783 (m), 733 (m) cm^{-1}.

UV/Vis: (CH_2Cl_2) λ_{max} (ε) 305 (30400) 380 (14000) 393 (15300) nm (M^{-1} cm^{-1}).

Fluorescence: (CH_2Cl_2) λ_{ex} = 380 nm, λ_{em} = 501 nm, PLQY: 0.03.

HRMS (MALDI, dctb): calcd. for $C_{56}H_{56}{}^{79}Br_2$: 886.2743 [M^+]; found: 886.2742.

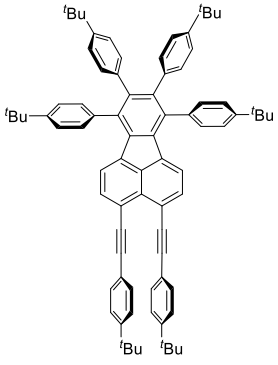

7,8,9,10-Tetrakis(4-*tert*-butylphenyl)-3,4-bis[(4-*tert*-butylphenyl)ethynyl]fluoranthene (4).

A mixture of **3** (40.0 mg, 45.0 µmol), 1-(*tert*-butyl)-4-ethynylbenzene (40.6 µL, 225 µmol), [$Pd(PPh_3)_4$] (2.60 mg, 2.25 µmol), copper(I) iodide (1.71 mg, 9.00 µmol) and triethylamine (5 mL) in a Schlenk tube at ambient temperature was purged with nitrogen for 10 min. The reaction mixture was stirred at 100 °C for 18 h. After cooling to rt, the mixture was extracted with CH_2Cl_2 (3×100 mL). The combined organic phases were washed with sat. aq. NH_4Cl (3×75 mL), dried over Na_2SO_4 and filtered. After removal of the solvent, the residue was purified via column chromatography (SiO_2, PE/CH_2Cl_2 10:1) and then recrystallized from hot $CHCl_3$ layered with MeOH to obtain compound **4** (28.8 mg, 27.6 µmol, 61%) as an orange solid.

M.p.: 344–346 °C (decomp.).

R_f = 0.48 (SiO_2, PE/CH_2Cl_2 3:1).

^{1}H NMR (600 MHz, CD_2Cl_2): δ = 7.57 (d, *J* = 7.5 Hz, 2H), 7.36 (dt, *J* = 8.4, 1.9 Hz, 4H), 7.25 (dt, *J* = 8.5, 1.8 Hz, 4H), 7.21 (dt, *J* = 8.2, 1.9 Hz, 4H), 7.18 (dt, *J* = 8.5, 2.0 Hz, 4H), 6.91 (dt, *J* = 8.4, 1.8 Hz, 4H), 6.82 (dt, *J* = 8.4, 2.1 Hz, 4H), 6.46 (d, *J* = 7.5 Hz, 2H), 1.34 (s, 18H), 1.27 (s, 18H), 1.12 (s, 18H) ppm.

^{13}C NMR (151 MHz, $CDCl_3$): δ = 151.9, 150.5, 148.5, 141.9, 137.9, 137.7, 137.5, 137.1, 136.3, 135.9, 133.8, 131.9, 131.3, 129.9, 128.5, 125.5, 123.7, 123.4, 120.8, 120.5, 97.1, 89.1, 35.0, 34.8, 34.4, 31.5, 31.3 ppm. (two signals are coincident or not observed)

IR (FT-ATR): $\tilde{\nu}$ = 3084 (w), 3063 (w), 3033 (m), 2956 (m), 2901 (m), 2867 (m), 1511 (m), 1461 (m), 1430 (m), 1392 (m), 1362 (m), 1268 (m), 1201 (m), 1117 (w), 1017 (m), 833 (s), 778 (m) cm^{-1}.

UV/Vis: (CH_2Cl_2) λ_{max} (ε) 309 (47400) 421 (33800) nm (M^{-1} cm^{-1}).

Fluorescence: (CH_2Cl_2) λ_{ex} = 420 nm, λ_{em} = 528 nm, PLQY: 0.45.

HRMS (MALDI, dctb): calcd. for $C_{80}H_{82}$: 1042.6411 [M^+]; found: 1042.6420.

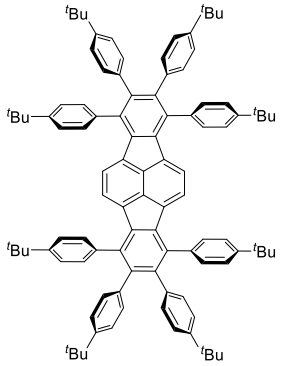

$C_{102}H_{108}$
1333.99 g/mol

1,2,3,4,7,8,9,10-Octakis(4-*tert*-butylphenyl)indeno[1,2,3-*cd*]fluoranthene (OPP).

A microwave tube was charged with dry *o*-xylene (2.00 mL), diyne **4** (10.0 mg, 9.58 µmol), bis(4-*tert*-butylphenyl)acetylene (2.78 mg, 9.58 µmol) and [$RhCl(PPh_3)_3$] (443 µg, 0.48 µmol) and the solution was deoxygenated with nitrogen. The sealed tube was maintained at 135 °C for 52 h. After cooling to rt, the solvent was removed under reduced pressure and the residue was recrystallized from hot $CHCl_3$ layered with MeOH to afford the desired compound **OPP** (11.1 mg, 8.32 µmol, 87%) as an orange solid.

M.p.: >400 °C.

R_f = 0.42 (SiO_2, PE/CH_2Cl_2 3:1).

^{1}H NMR (600 MHz, $CDCl_3$, 50 °C): δ = 7.21 (d, *J* = 8.3 Hz, 8H), 7.12 (d, *J* = 8.2 Hz, 8H), 6.82 (d, *J* = 8.4 Hz, 8H), 6.70 (d, *J* = 8.4 Hz, 8H), 6.03 (s, 4H), 1.25 (s, 36H), 1.08 (s, 36H) ppm.

^{13}C NMR (151 MHz, $CDCl_3$, 50 °C): δ = 149.6, 148.0, 141.7, 139.3, 138.3, 137.4, 137.1, 137.0, 133.4, 131.0, 129.7, 124.8, 124.5, 123.3, 34.6, 34.2, 31.5, 31.3 ppm.

IR (FT-ATR): $\tilde{\nu}$ = 3081 (m), 3055 (m), 3033 (m), 2956 (m), 2901 (m), 2864 (m), 1901 (m), 1513 (m), 1461 (m), 1416 (m), 1392 (m), 1360 (m), 1322 (m), 1268 (m), 1234 (w), 1198 (m), 1169 (m), 1112 (m), 1048 (m), 1015 (m), 921 (m), 829 (m), 778 (m), 742 (m), 715 (m) cm^{-1}.

UV/Vis: (CH_2Cl_2) λ_{max} (ε) 314 (58500) 397 (12200) 419 (24900) 445 (29800) nm (M^{-1} cm^{-1}).

HRMS (MALDI, dctb): calcd. for $C_{102}H_{108}$: 1332.8446 [M^+]; found: 1332.8456.

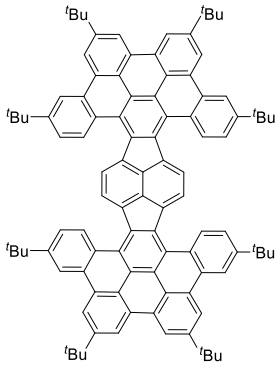

$C_{102}H_{96}$
1321.89 g/mol

HBC-Pyracylene Hybrid (HPH).

Route A: Compound **OPP** (10.0 mg, 7.50 µmol) and DDQ (11.2 mg, 49.5 µmol) were dissolved in dry CH_2Cl_2 (10 mL). The solution was cooled to 0 °C and deoxygenated with nitrogen for 10 min. To the cooled solution was added TfOH (100 µL, 1.14 mmol, 1 v%) dropwise over 5 min. After additional 15 min of stirring at this temperature, the reaction mixture was quenched *via* dropwise addition of sat. aq. Na_2CO_3 (10 mL). The reaction mixture was extracted with CH_2Cl_2 (3×75 mL), dried over Na_2SO_4 and filtered. The solvent was evaporated under reduced pressure to give compound **HPH** (9.90 mg, 7.49 µmol, 99%) as a deep purple solid.

Route B: Compound **TPP** (25.0 mg, 37.7 µmol) and DDQ (28.2 mg, 124 µmol) were dissolved in dry CH_2Cl_2 (25 mL). The solution was cooled to 0 °C and deoxygenated with nitrogen for 10 min. To the cooled solution was added TfOH (250 µL, 2.85 mmol, 1 v%) dropwise over 5 min. After additional 15 min of stirring at this temperature, the reaction mixture was quenched *via* dropwise addition of sat. aq. Na_2CO_3 (10 mL). The reaction was extracted with CH_2Cl_2 (3×75 mL), dried over Na_2SO_4 and filtered. The solvent was evaporated under reduced pressure to give compound **HPH** (24.7 mg, 18.7 µmol, 99%) as a deep purple solid.

M.p.: >400 °C.

R_f = 0.54 (SiO_2, PE/CH_2Cl_2 3:1).

^{1}H NMR (700 MHz, CD_2Cl_2): δ = 9.43 (s, 4H), 9.04 (s, 4H), 8.90 (s, 4H), 8.72 (s, 4H), 8.12 (s, 4H), 7.77 (s, 4H), 1.68 (s, 36H), 1.58 (s, 36H) ppm.

^{13}C NMR (151 MHz, $CDCl_3$, 50 °C): δ = 151.2, 149.2, 141.5, 135.4, 135.2, 131.7, 130.5, 130.0, 129.3, 128.0, 126.5, 124.9, 124.5, 123.9, 123.2, 120.1, 118.9, 118.7, 35.7, 35.4, 32.0, 31.8 ppm.

IR (FT-ATR): $\tilde{\nu}$ = 3077 (w), 2954 (m), 2924 (m), 2864 (m), 1609 (m), 1581 (m), 1458 (m), 1390 (m), 1362 (m), 1254 (m), 1201 (m), 1153 (m), 1117 (m), 1020 (m), 978 (m), 932 (m), 869 (m), 824 (m), 785 (m), 737 (m), 621 (m) cm^{-1}.

UV/Vis: (CH_2Cl_2) λ_{max} (ε) 400 (69800) 422 (104900) 419 (24900) 508 (9400) 546 (20200) 587 (25500) nm (M^{-1} cm^{-1}).

HRMS (MALDI, dctb): calcd. for $C_{102}H_{96}$: 1320.7507 [M^+]; found: 1320.7530.

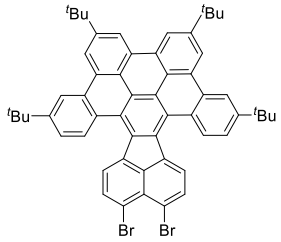

$C_{56}H_{50}Br_2$
882.82 g/mol

3,4-Dibromo-9,12,15,18-tetra-*tert*-butyldibenzo[*fg*,*ij*]fluorantheno[7,8,9,10-*rst*]pentaphene (5).

Compound **3** (200 mg, 225 µmol) and DDQ (169 mg, 743 µmol) were dissolved in dry CH_2Cl_2 (200 mL). The solution was cooled to 0 °C and deoxygenated with nitrogen for 10 min. To the cooled solution was added TfOH (2.00 mL, 22.8 mmol, 1 v%) dropwise over 5 min. After additional 15 min of stirring at this temperature, the reaction mixture was quenched *via* dropwise addition of sat. aq. Na_2CO_3 (50 mL). The reaction was extracted with CH_2Cl_2 (3×100 mL), dried over Na_2SO_4 and filtered. The solvent was evaporated under reduced pressure to give the crude material which was purified by column chromatography to obtain **5** (192 mg, 218 µmol, 97%) as an orange solid.

M.p.: >400 °C.

R_f = 0.72 (SiO_2, PE/CH_2Cl_2 3:1).

^{1}H NMR (400 MHz, CD_2Cl_2): δ = 9.24 (d, *J* = 8.5 Hz, 2H), 9.13 (s, 2H), 8.99 (s, 2H), 8.79 (d, *J* = 1.5 Hz, 2H), 8.55 (d, *J* = 7.9 Hz, 2H), 7.89 (d, *J* = 7.9 Hz, 2H), 7.74 (dd, *J* = 8.5, 1.7 Hz, 2H), 1.74 (s, 18H), 1.61 (s, 18H) ppm.

^{13}C NMR (101 MHz, CD_2Cl_2): δ = 152.0, 150.1, 139.4, 135.9, 135.6, 132.4, 131.8, 130.6, 130.0, 129.3, 127.4, 127.3, 125.9, 124.4, 124.3, 124.2, 122.9, 120.5, 120.3, 119.6, 119.2, 36.0, 35.7, 32.0, 31.7 ppm.

IR (FT-ATR): $\tilde{\nu}$ = 2948 (m), 2902 (w), 2866 (w), 2359 (w), 1608 (m), 1392 (m), 1258 (m), 1185 (m), 1151 (m), 1059 (m), 1022 (m), 966 (m), 929 (m), 823 (m) cm^{-1}.

UV/Vis: (CH_2Cl_2) λ_{max} (ε) 314 (30400) 330 (32100) 343 (25300) 372 (37500) 391 (68500) 452 (4800) 480 (8400) 510 (10000) nm (M^{-1} cm^{-1}).

Fluorescence: (CH_2Cl_2) λ_{ex} = 395 nm, λ_{em} = 552, 583 nm, PLQY: 0.05.

HRMS (MALDI, dctb): calcd. for $C_{56}H_{50}{}^{79}Br_2$: 880.2274 [M^+]; found: 880.2283.

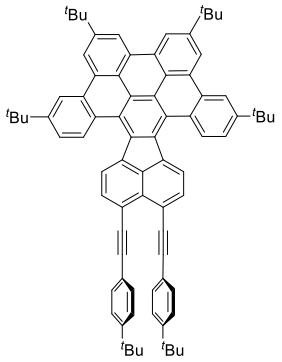

9,12,15,18-Tetra-*tert*-butyl-3,4-bis[(4-*tert*-butylphenyl)ethynyl]dibenzo[*fg*,*ij*]fluoranthene [7,8,9,10-*rst*]pentaphene (6).

A mixture of **5** (75.0 mg, 85.0 µmol), 1-(*tert*-butyl)-4-ethynylbenzene (61.3 µL, 340 µmol), [Pd(PPh$_3$)$_4$] (4.91 mg, 4.25 µmol), copper(I) iodide (3.24 mg, 17.0 µmol), triethylamine (4 mL), THF (1 mL) and toluene (1 mL) in a Schlenk tube at ambient temperature was purged with nitrogen for 10 min. The reaction mixture was stirred at 100 °C for 36 h. After cooling to rt, the mixture was extracted with CH_2Cl_2 (3×100 mL). The combined organic phases were washed with sat. aq. NH_4Cl solution (3×75 mL), dried over Na_2SO_4 and filtered. After removal of the solvent, the residue was purified via column chromatography (SiO_2, PE/CH_2Cl_2 5:1) to obtain compound **6** (85.2 mg, 82.1 µmol, 97%) as a red solid.

M.p.: 256–257 °C (decomp).

R_f = 0.53 (SiO_2, PE/CH_2Cl_2 3:1).

^{1}H NMR (600 MHz, $CDCl_3$, 50 °C): δ = 9.36 (d, *J* = 8.5 Hz, 2H), 9.10 (d, *J* = 1.2 Hz, 2H), 8.97 (d, *J* = 1.2 Hz, 2H), 8.78 (d, *J* = 1.7 Hz, 2H), 8.74 (d, *J* = 7.6 Hz, 2H), 7.84 (d, *J* = 7.6 Hz, 2H), 7.73 (dd, *J* = 8.5, 1.9 Hz, 2H), 7.34 (d, *J* = 8.5 Hz, 4H), 7.19 (d, *J* = 8.5 Hz, 4H), 1.75 (s, 18H), 1.63 (s, 18H), 1.31 (s, 18H) ppm.

^{13}C NMR (151 MHz, $CDCl_3$, 50 °C): δ = 151.5, 151.4, 149.4, 138.8, 135.4, 133.2, 133.0, 131.9, 131.6, 130.5, 130.0, 129.6, 129.1, 127.7, 126.1, 125.1, 124.2, 123.7, 123.1, 123.1, 121.4, 121.1, 120.1, 119.1, 118.8, 97.7, 89.4, 35.8, 35.5, 34.9, 32.1, 31.8, 31.4 ppm.

IR (FT-ATR): $\tilde{\nu}$ = 3077 (w), 3037 (w), 2954 (s), 2903 (m), 2867 (m), 1607 (m), 1579 (m), 1506 (m), 1461 (m), 1428 (m), 1390 (m), 1362 (m), 1308 (m), 1258 (m), 1201 (m), 1153 (m), 1110 (m), 1081 (m), 1020 (m), 928 (m), 871 (m), 829 (s), 790 (m), 735 (m) cm^{-1}.

UV/Vis: (CH_2Cl_2) λ_{max} (ε) 282 (61000) 319 (43400) 335 (43400) 396 (58400) 412 (80400) 475 (11700) 504 (19400) 538 (20600) nm (M^{-1} cm^{-1}).

Fluorescence: (CH_2Cl_2) λ_{ex} = 413 nm, λ_{em} = 580, 616 nm, PLQY: 0.49.

HRMS (MALDI, dctb): calcd. for $C_{80}H_{76}$: 1036.5942 [M$^+$]; found: 1036.5953.

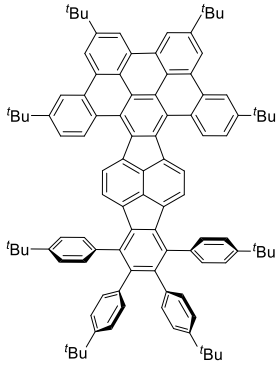

$C_{102}H_{102}$
1327.94 g/mol

9,12,15,18-Tetra-*tert*-butyl-1,2,3,4-tetrakis(4-*tert*-butylphenyl)dibenzo[*fg*,*ij*]indeno [1',2',3':3,4]fluorantheno[7,8,9,10-*rst*]pentaphene (TPP).

A microwave tube was charged with dry *o*-xylene (15.0 mL), diyne **6** (200.0 mg, 193 µmol), bis(4-*tert*-butylphenyl)acetylene (56.0 mg, 193 µmol) and [$RhCl(PPh_3)_3$] (8.92 mg, 9.64 µmol) and the solution was deoxygenated with nitrogen. The sealed tube was maintained at 135 °C for 52 h. After cooling to rt, the solvent was removed under reduced pressure and the residue was purified via column chromatography (SiO_2, PE/CH_2Cl_2 5:1) to obtain compound **TPP** (197 mg, 148 µmol, 77%) as a red solid.

M.p.: >400 °C.

R_f = 0.52 (SiO_2, PE/CH_2Cl_2 3:1).

^{1}H NMR (600 MHz, CD_2Cl_2): δ = 9.19 (d, *J* = 8.4 Hz, 2H), 9.08 (d, *J* = 1.1 Hz, 2H), 8.92 (d, *J* = 1.2 Hz, 2H), 8.72 (d, *J* = 1.7 Hz, 2H), 7.97 (d, *J* = 7.5 Hz, 2H), 7.70 (dd, *J* = 8.4, 1.9 Hz, 2H), 7.32 (d, *J* = 7.8 Hz, 4H), 7.18 (d, *J* = 7.2 Hz, 4H), 6.89 (d, *J* = 8.4 Hz, 4H), 6.78 (d, *J* = 8.4 Hz, 4H), 6.15 (d, *J* = 7.5 Hz, 2H), 1.71 (s, 18H), 1.56 (s, 18H), 1.32 (s, 18H), 1.11 (s, 18H) ppm.

^{13}C NMR (151 MHz, CD_2Cl_2): δ = 151.7, 150.2, 149.7, 148.5, 142.1, 139.6, 139.0, 138.8, 138.5, 137.4, 137.1, 135.8, 134.6, 133.8, 131.5, 131.2, 130.5, 130.0, 129.8, 129.2, 127.8, 126.9, 125.2, 124.6, 124.5, 124.2, 123.7, 123.1, 120.1, 119.4, 119.1, 35.9, 35.5, 34.8, 34.4, 31.9, 31.6, 31.5, 31.3 ppm. (one signal is coincident or not observed)

IR (FT-ATR): $\tilde{\nu}$ = 2954 (s), 2903 (m), 2867 (m), 1607 (m), 1581 (m), 1509 (m), 1473 (m), 1461 (m), 1392 (m), 1358 (m), 1322 (m), 1261 (m), 1248 (m), 1200 (m), 1177 (m), 1149 (m), 1114 (m), 1044 (m), 1017 (m), 978 (m), 928 (m), 871 (m), 829 (s), 781 (m), 768 (m), 745 (m), 719 (m) cm^{-1}.

UV/Vis: (CH_2Cl_2) λ_{max} (ε) 308 (45600) 320 (50400) 343 (39400) 385 (40400) 402 (55800) 419 (44200) 472 (7400) 506 (15300) 539 (18000) nm (M^{-1} cm^{-1}).

HRMS (MALDI, dctb): calcd. for $C_{102}H_{102}$: 1326.7976 [M^+]; found: 1326.7991.

3. ^{1}H and ^{13}C Nuclear Magnetic Resonance Spectra

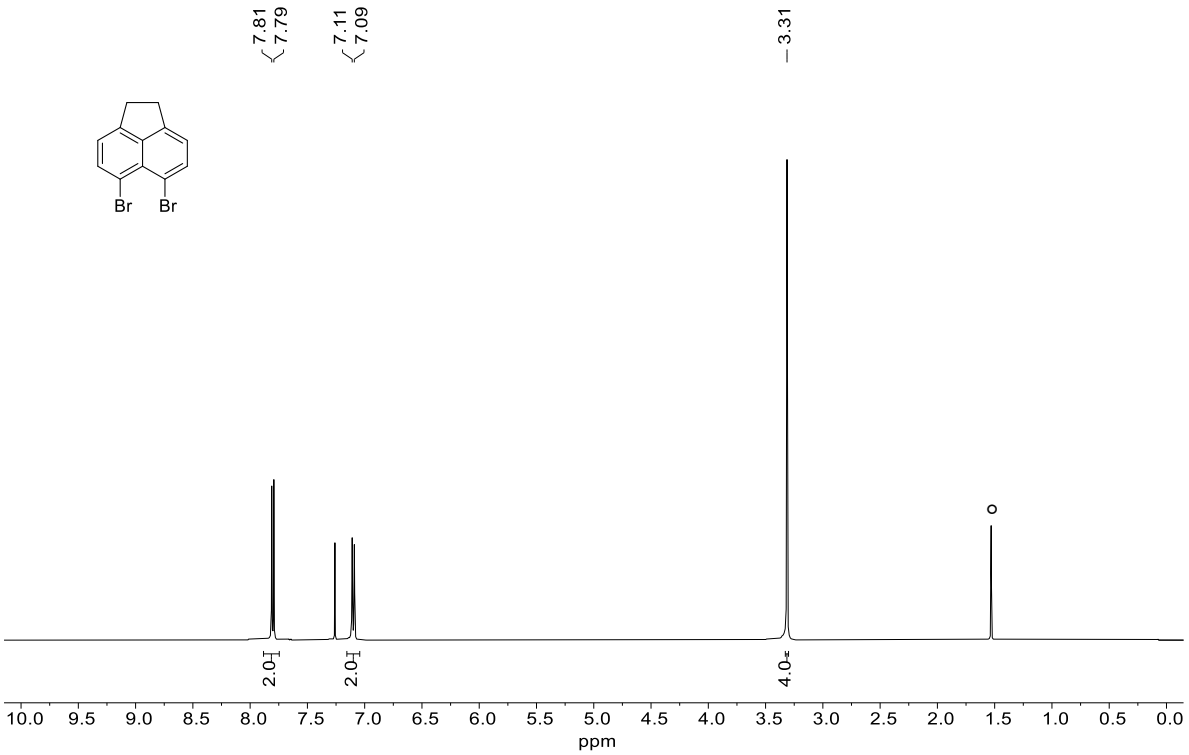

Figure S2: ^{1}H NMR spectrum of **S1** ($CDCl_3$, 400 MHz); °H_2O.

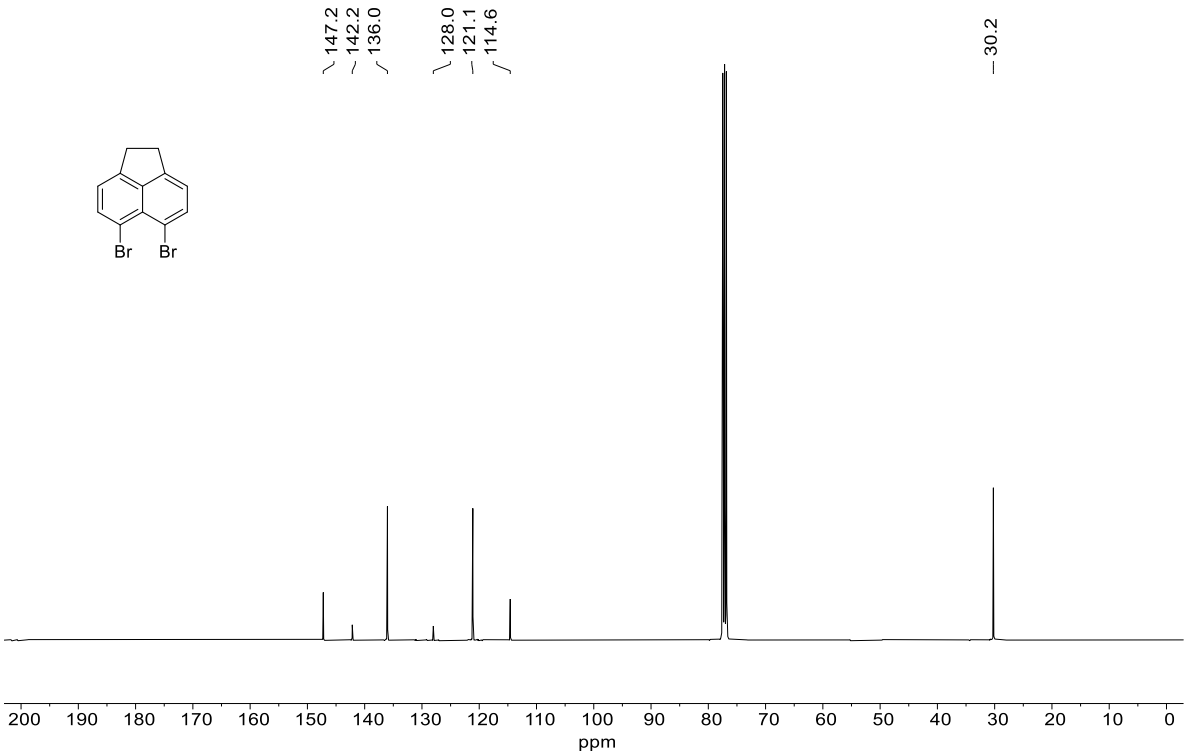

Figure S3: ^{13}C NMR spectrum of **S1** ($CDCl_3$, 101 MHz).

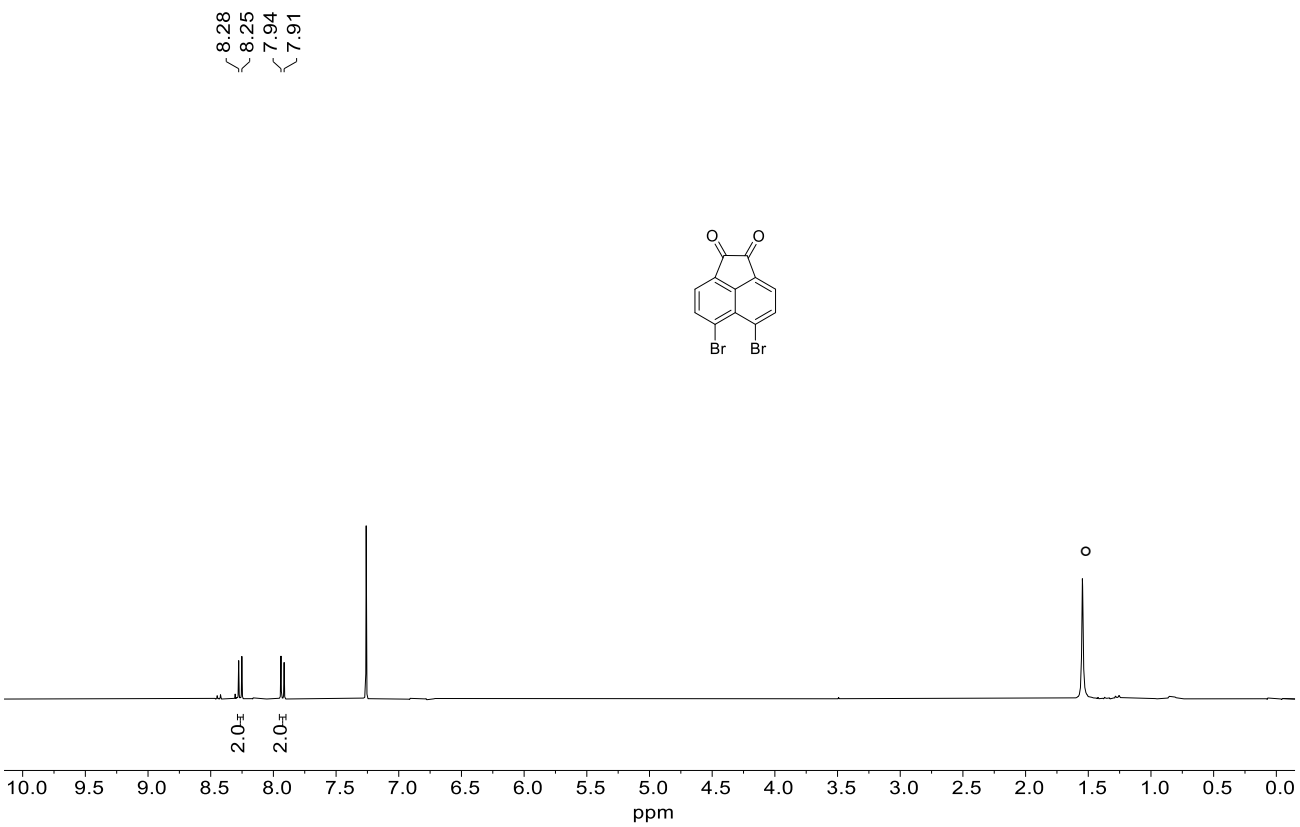

Figure S4: ^{1}H NMR spectrum of **S2** ($CDCl_3$, 300 MHz); $°H_2O$.

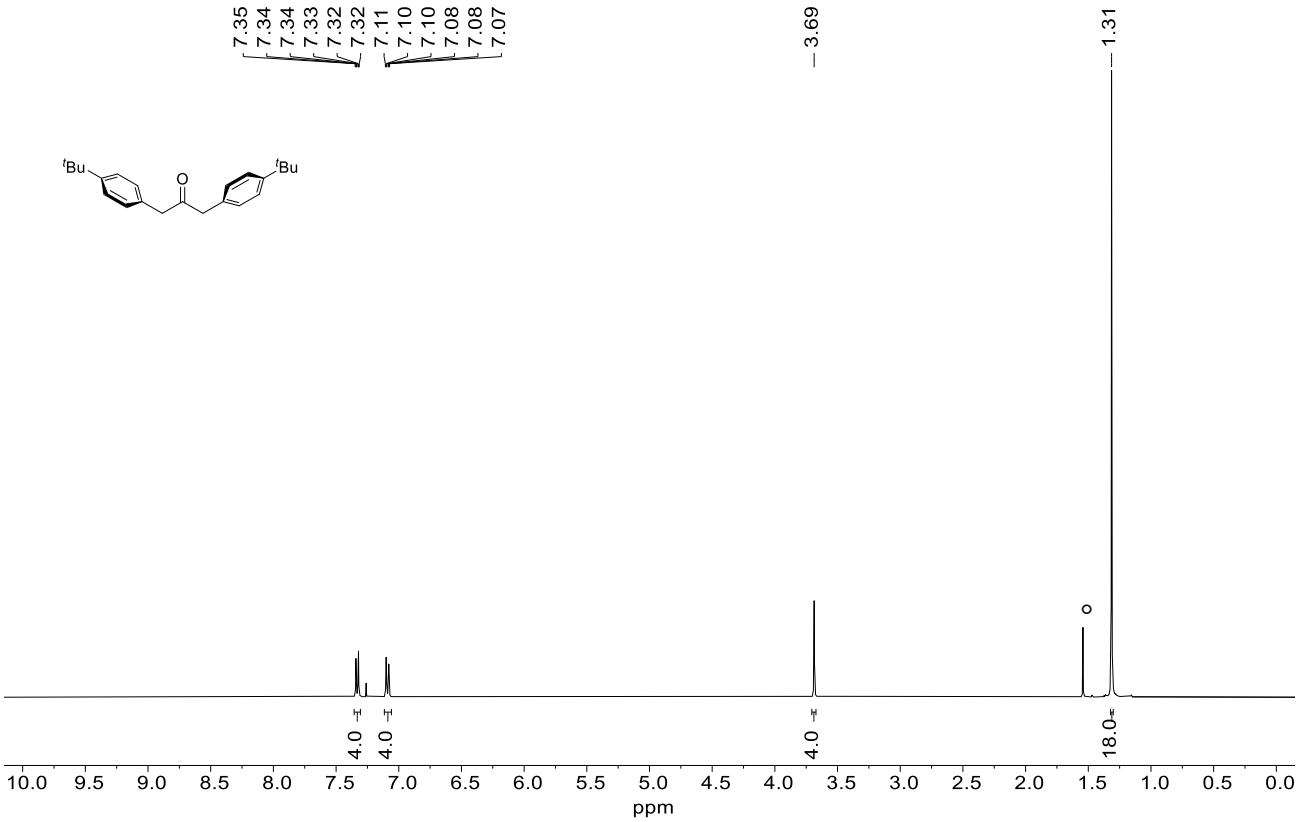

Figure S5: ^{1}H NMR spectrum of **S3** ($CDCl_3$, 400 MHz); °H_2O.

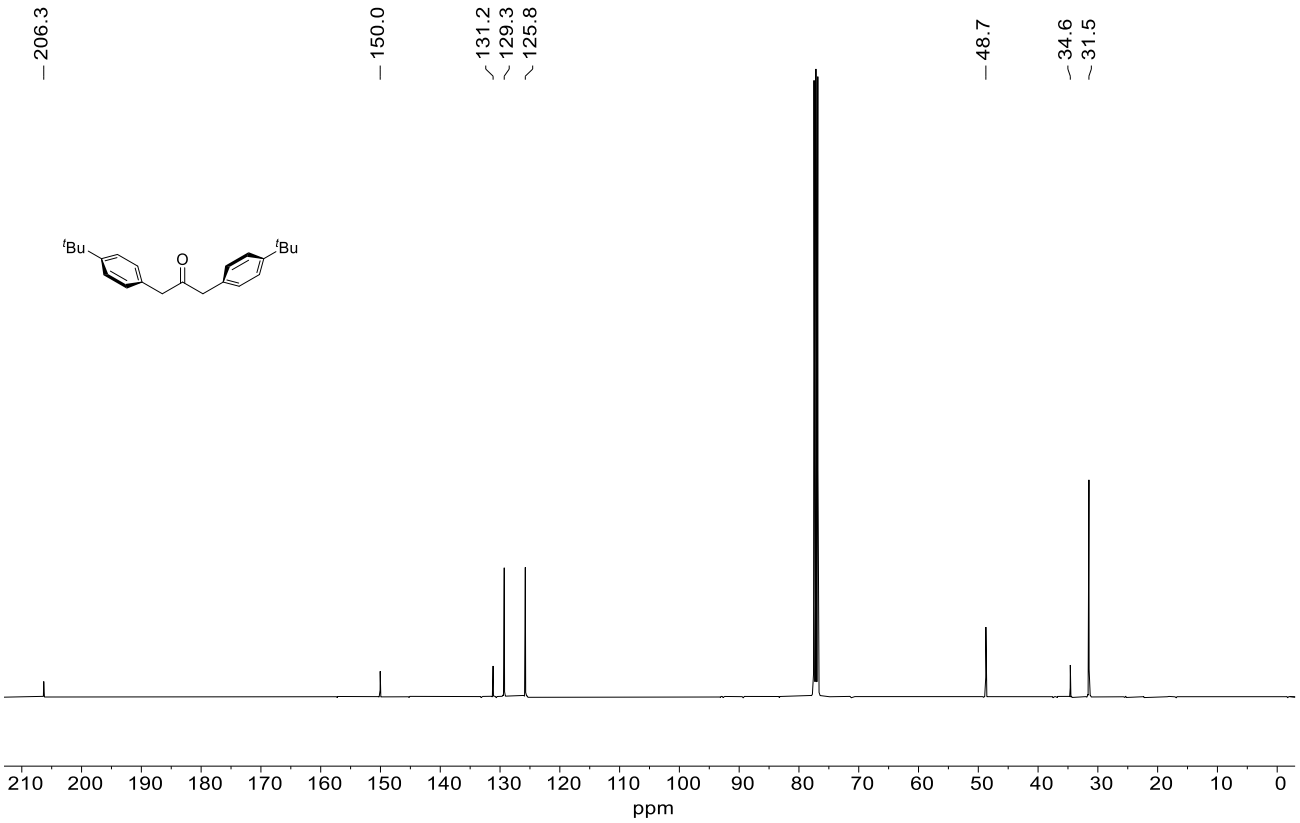

Figure S6: ^{13}C NMR spectrum of **S3** ($CDCl_3$, 101 MHz).

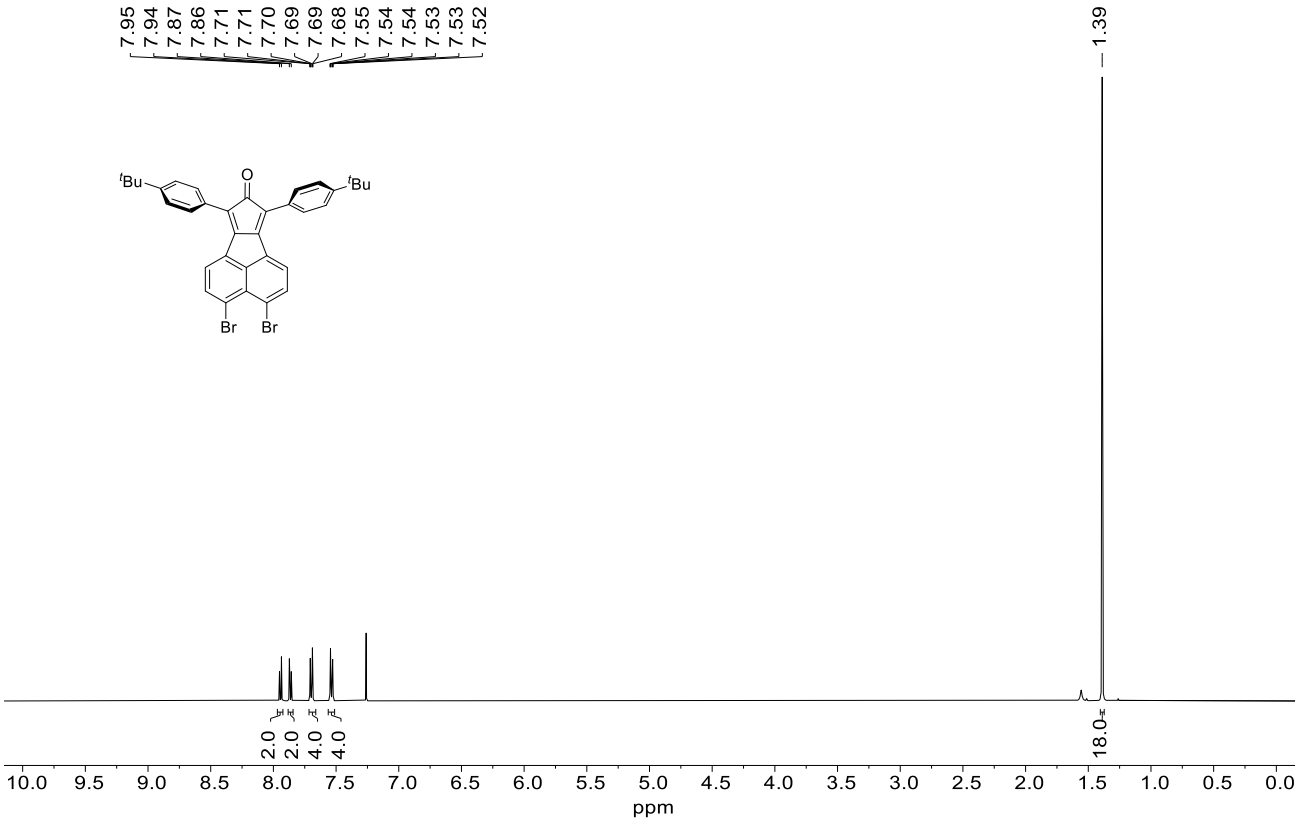

Figure S7: ^{1}H NMR spectrum of **S4** ($CDCl_3$, 500 MHz).

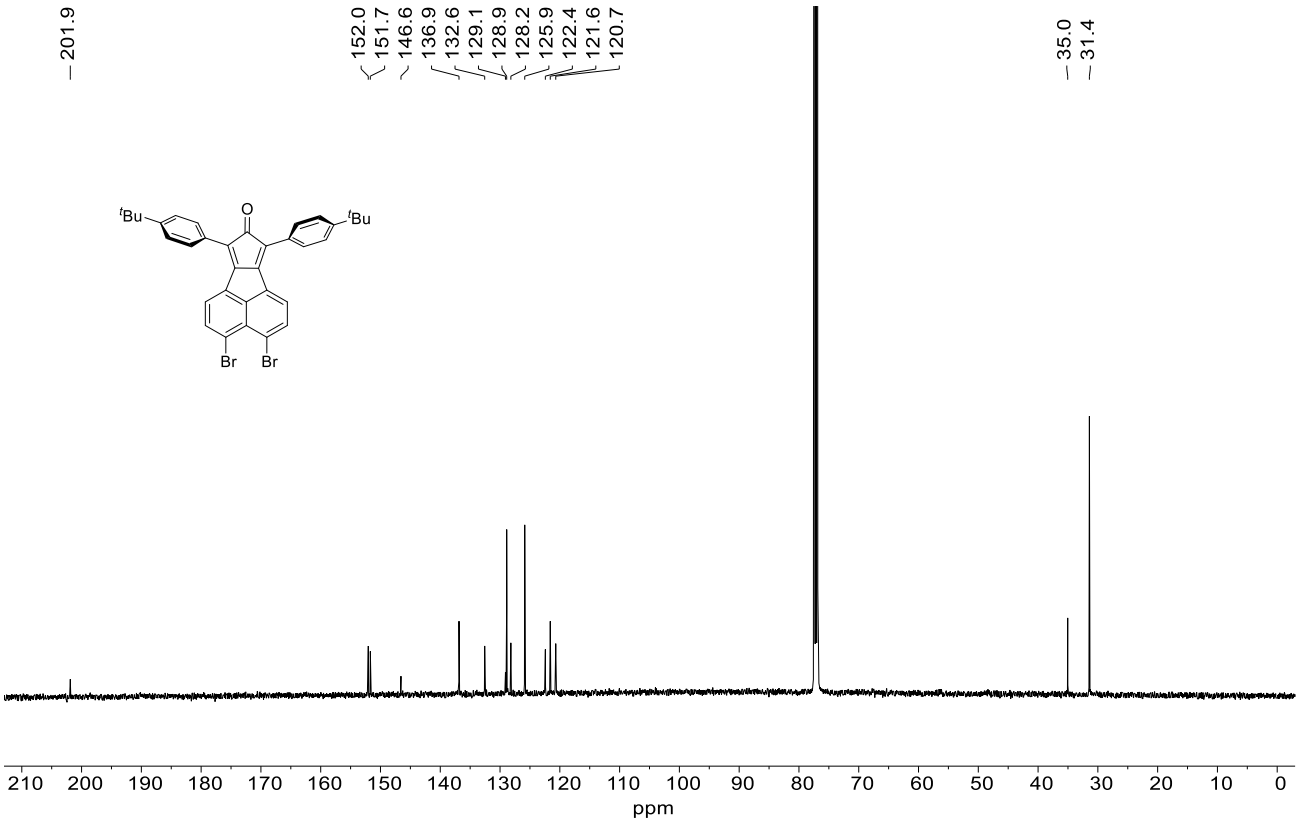

Figure S8: ^{13}C NMR spectrum of **S4** ($CDCl_3$, 126 MHz).

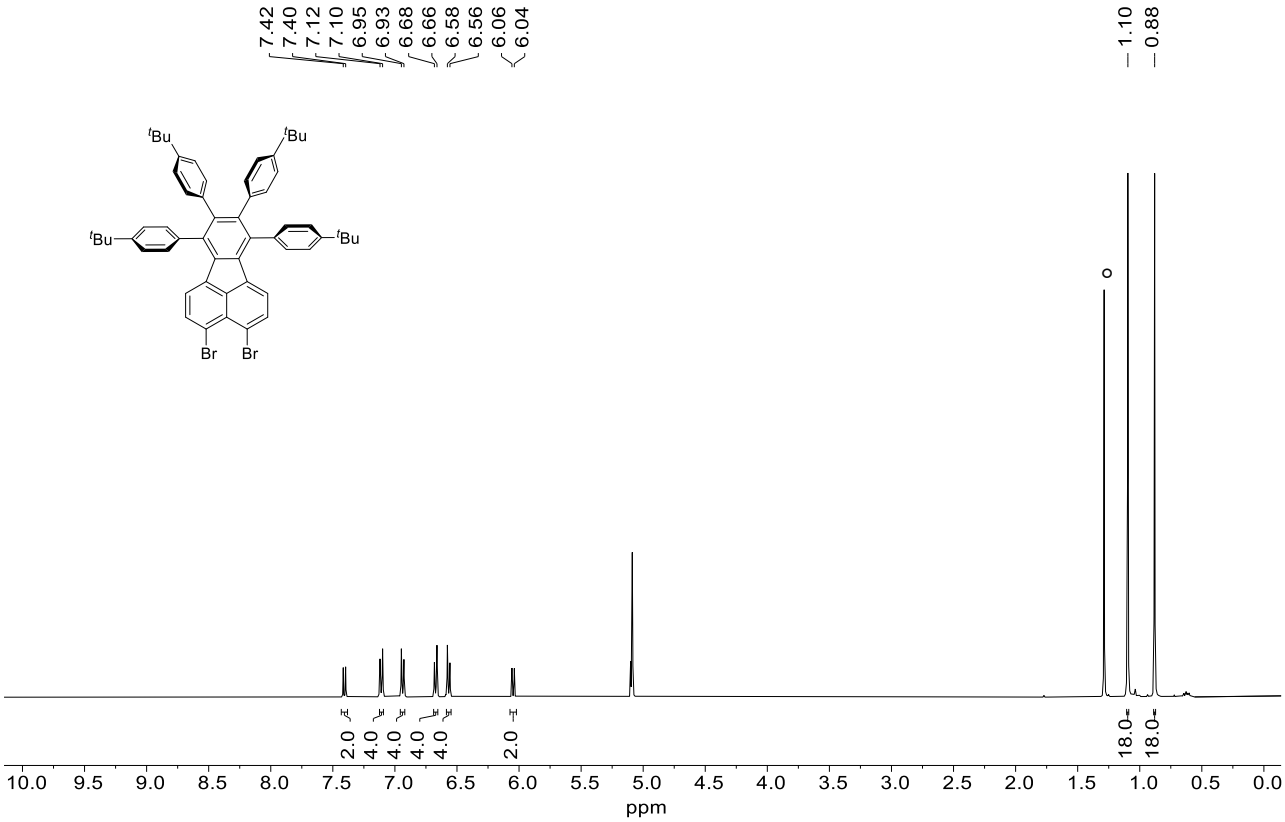

Figure S9: ^{1}H NMR spectrum of **3** (CD_2Cl_2, 400 MHz); °H_2O.

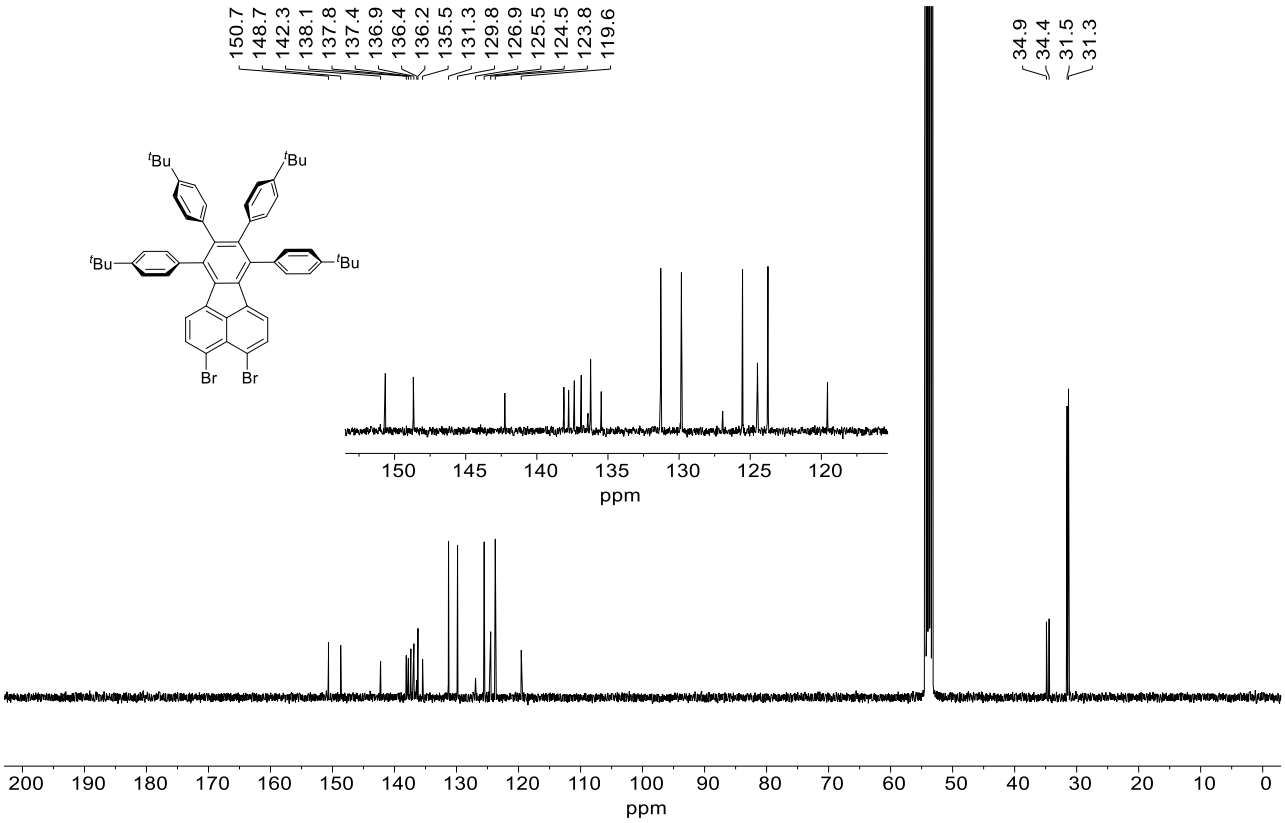

Figure S10: ^{13}C NMR spectrum of **3** (CD_2Cl_2, 101 MHz).

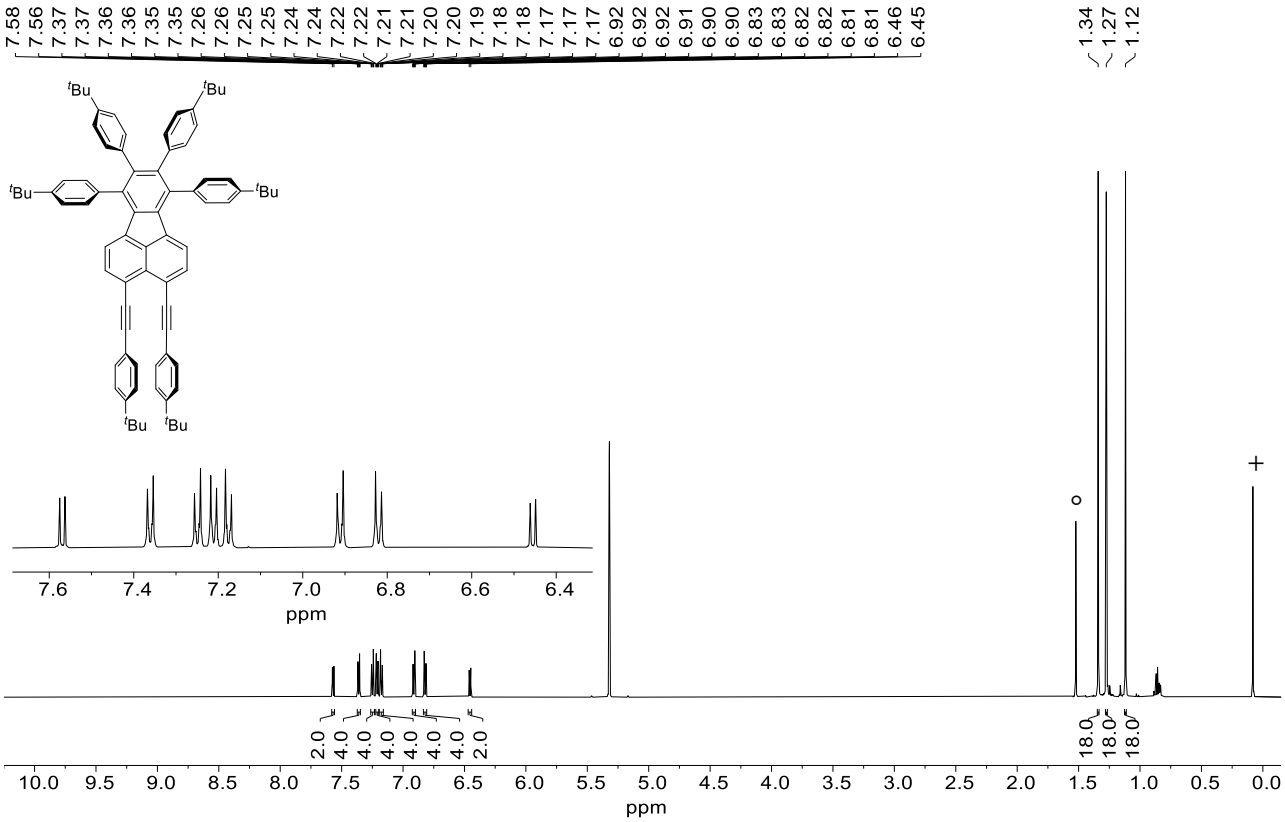

Figure S11: ^{1}H NMR spectrum of **4** (CD_2Cl_2, 600 MHz); °H_2O, $^{+}$silicone grease.

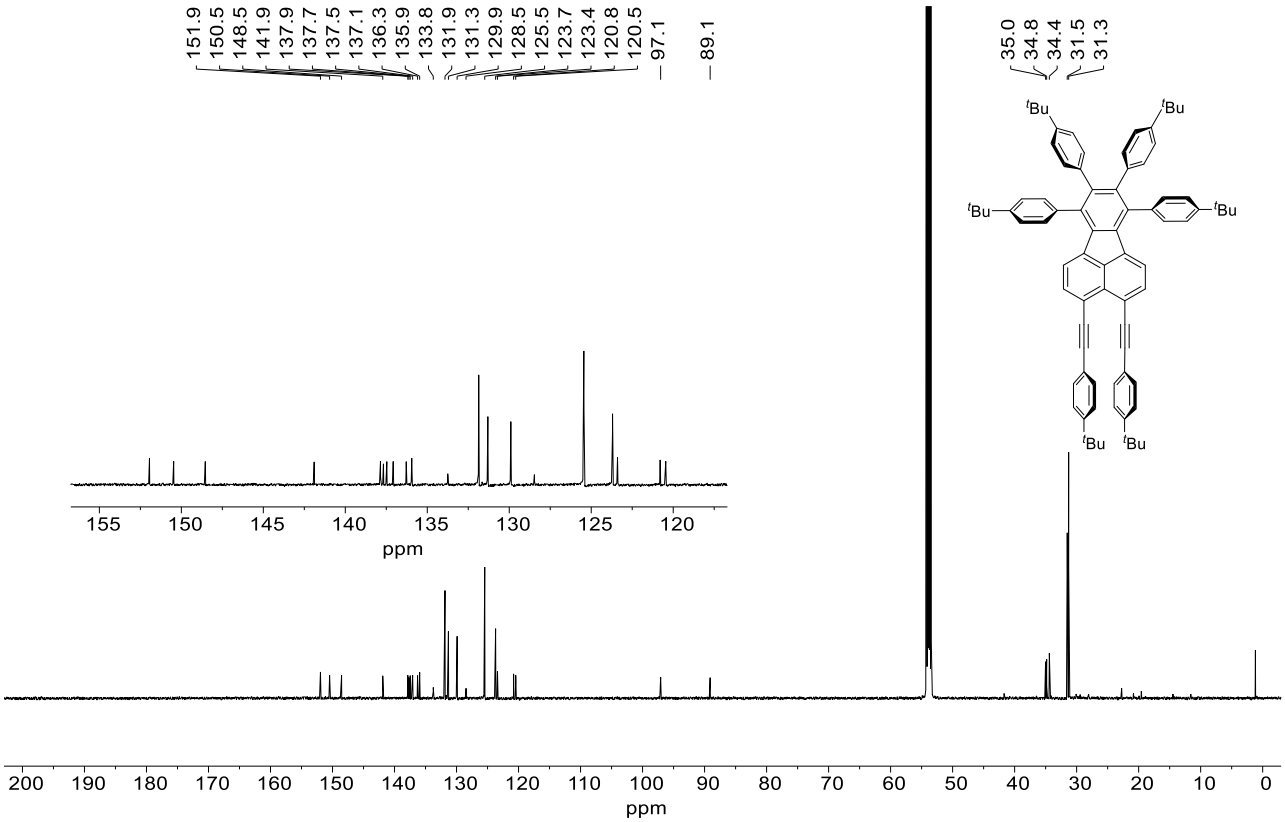

Figure S12: ^{13}C NMR spectrum of **4** (CD_2Cl_2, 151 MHz).

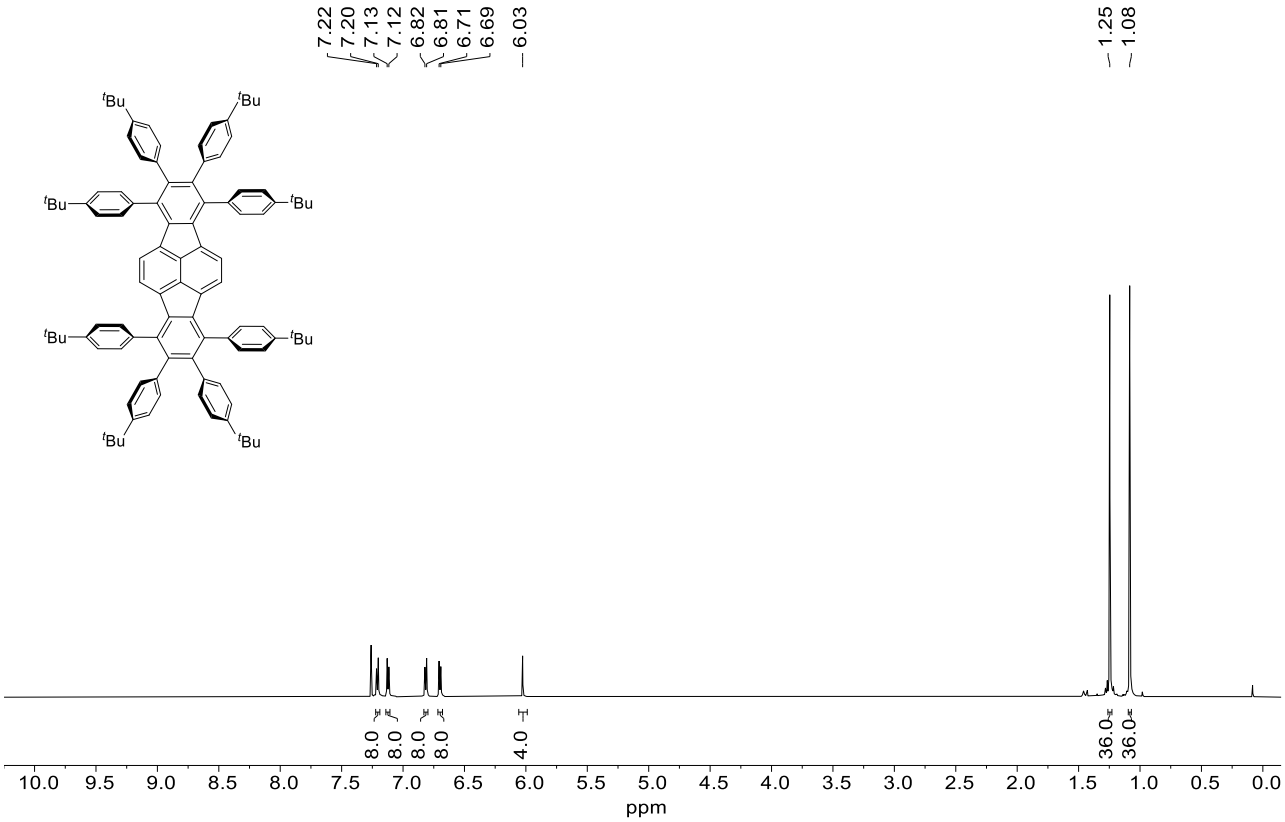

Figure S13: ^{1}H NMR spectrum of **OPP** ($CDCl_3$, 600 MHz, 50 °C).

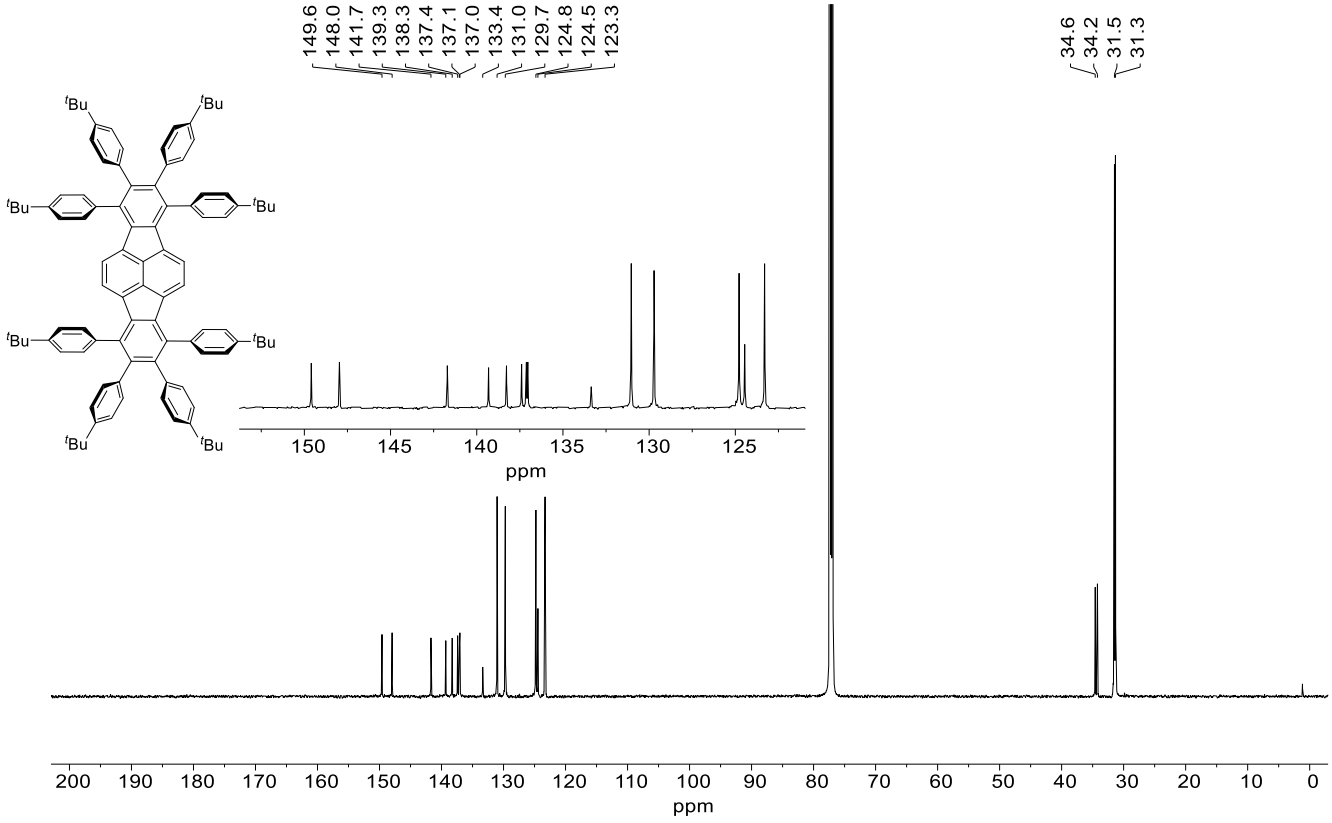

Figure S14: ^{13}C NMR spectrum of **OPP** ($CDCl_3$, 151 MHz, 50 °C).

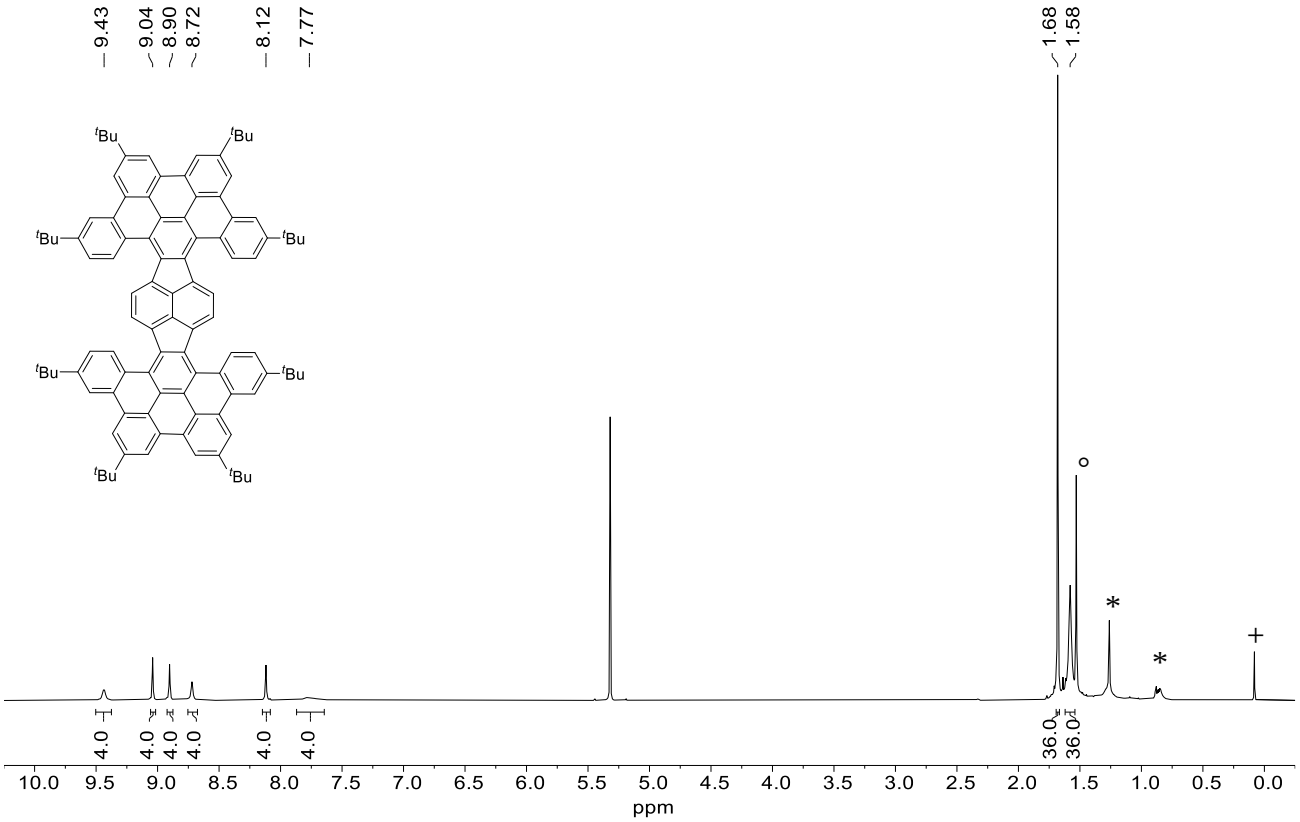

Figure S15: ^{1}H NMR spectrum of **HPH** (CD_2Cl_2, 700 MHz); °H_2O; *grease; $^{+}$silicone grease.

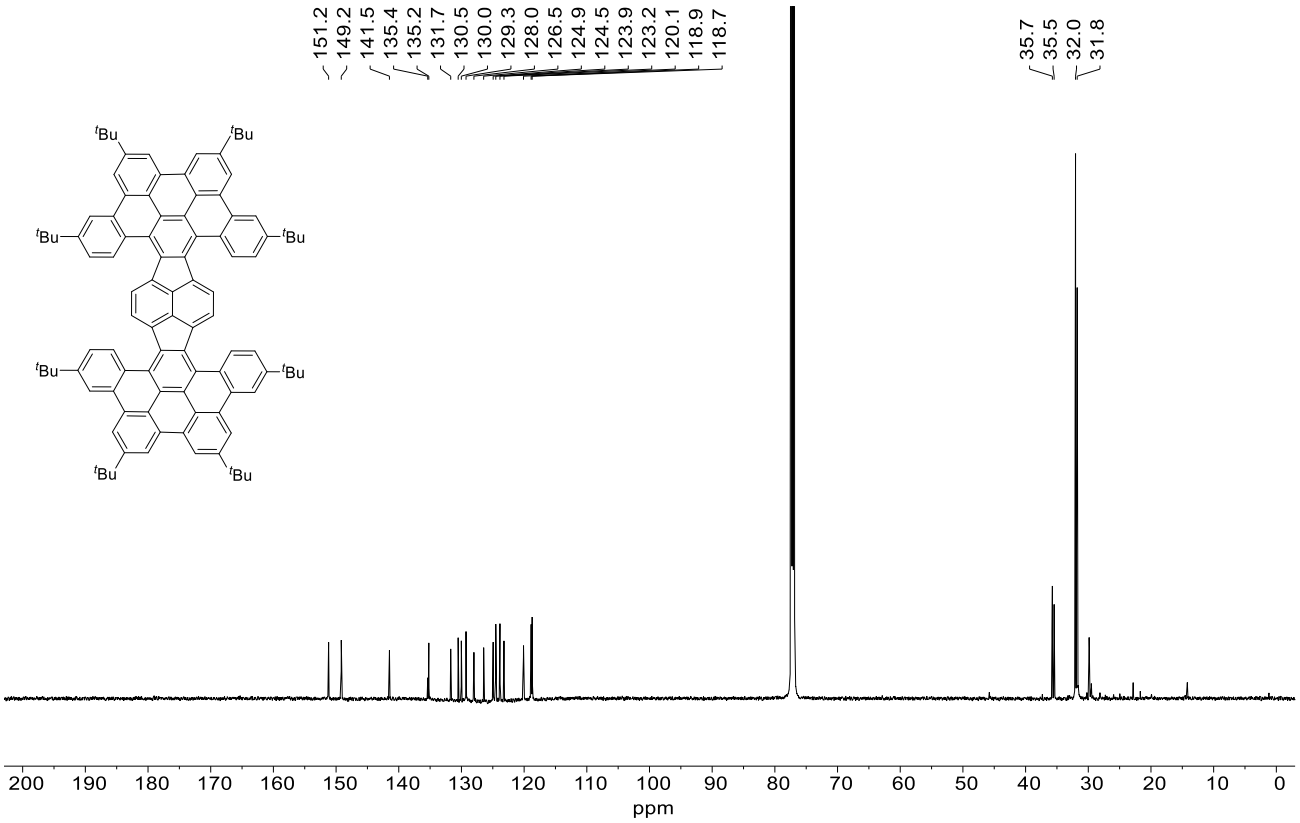

Figure S16: ^{13}C NMR spectrum of **HPH** ($CDCl_3$, 151 MHz).

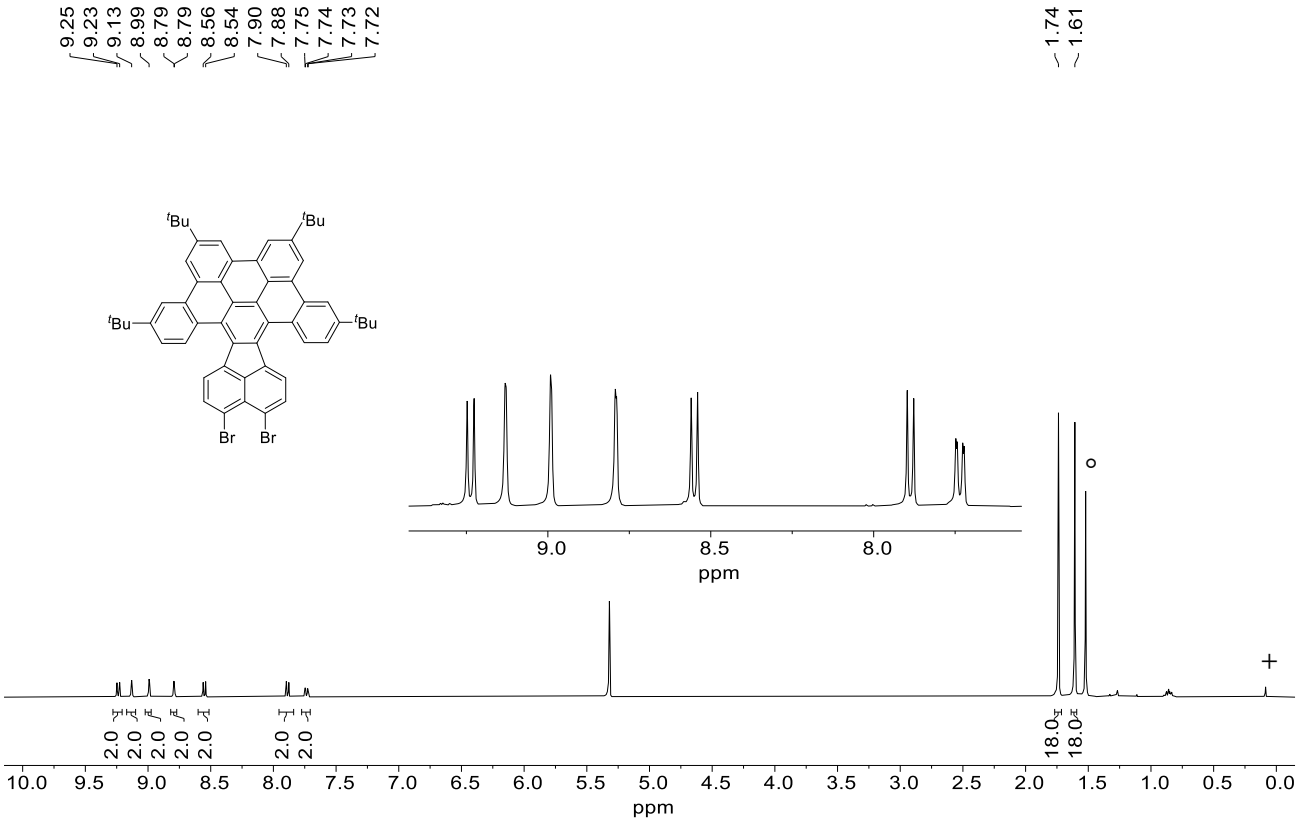

Figure S17: ^{1}H NMR spectrum of **5** (CD_2Cl_2, 400 MHz); °H_2O, $^{+}$silicone grease.

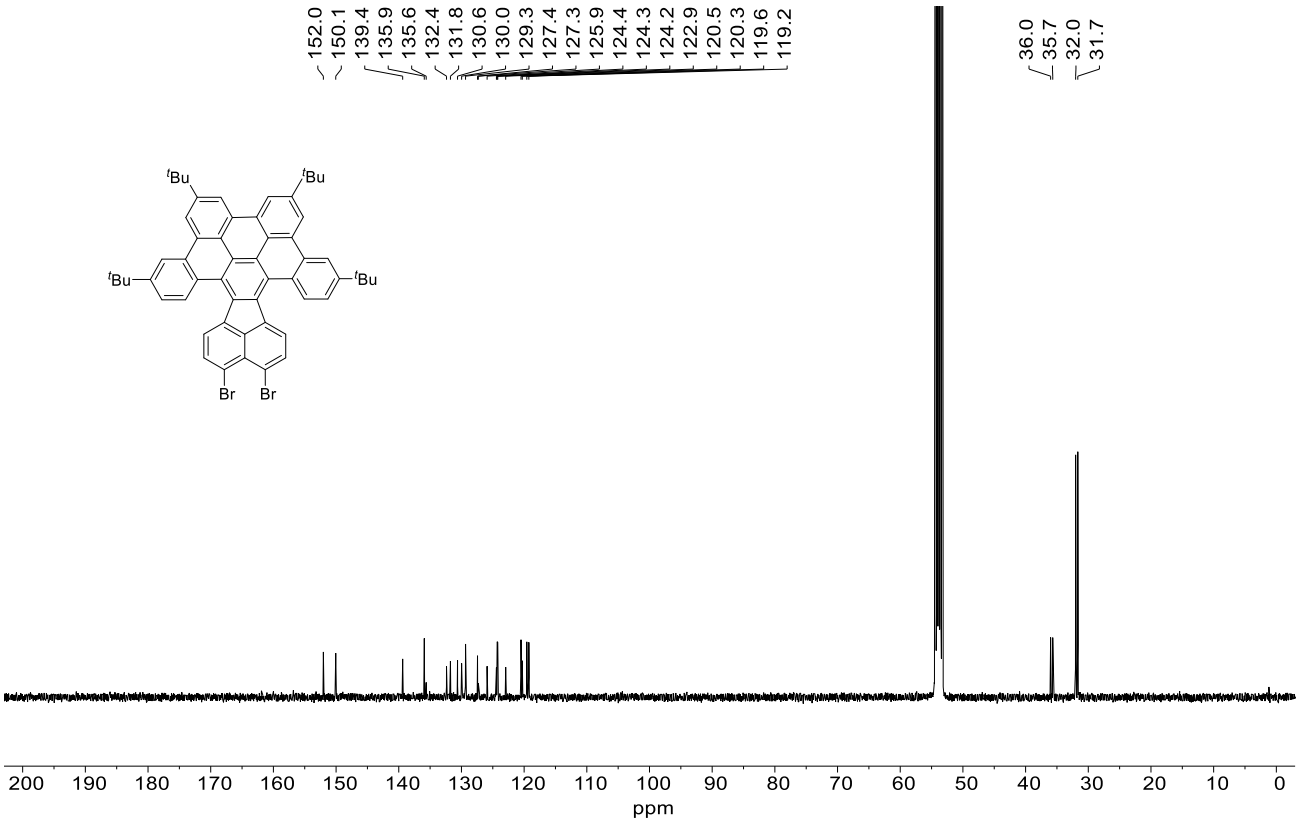

Figure S18: ^{13}C NMR spectrum of **5** (CD_2Cl_2, 101 MHz).

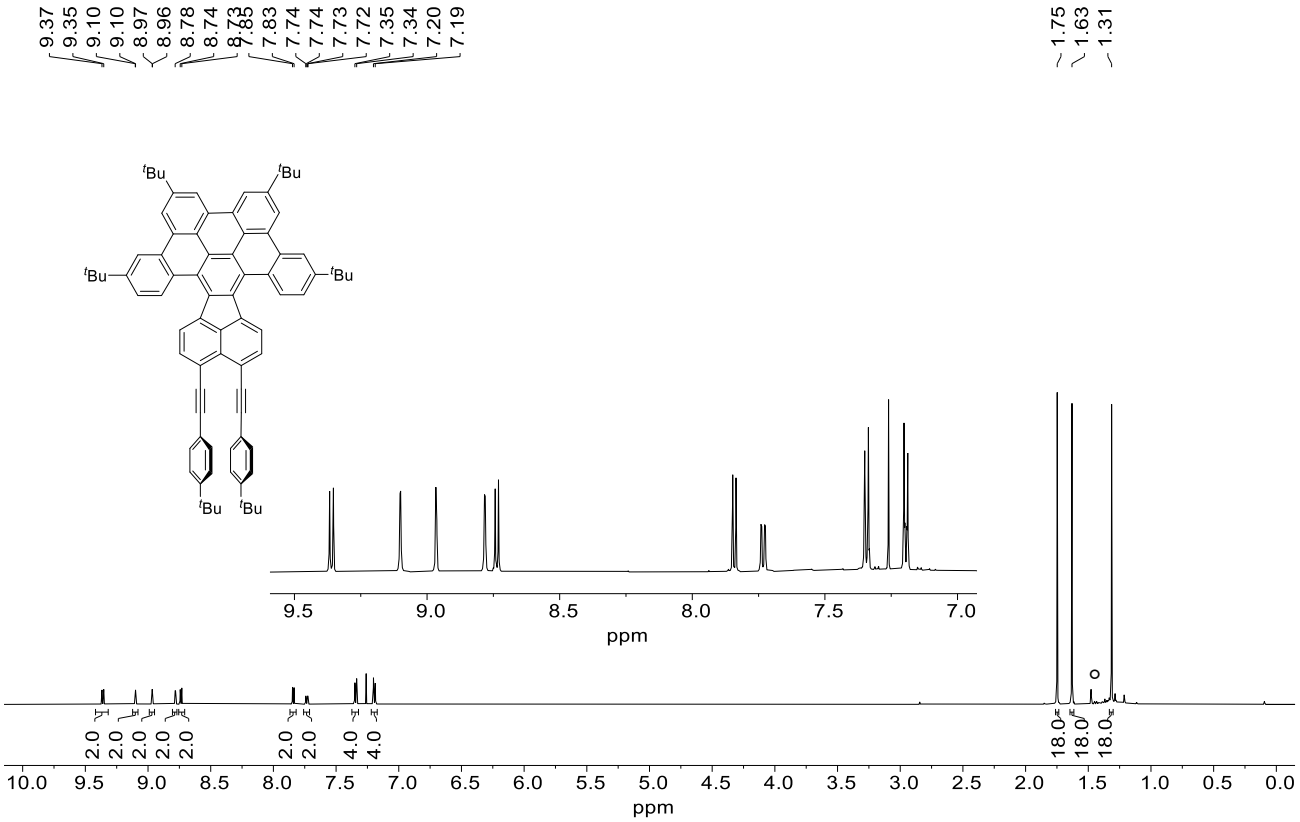

Figure S19: ^{1}H NMR spectrum of **6** ($CDCl_3$, 600 MHz, 50 °C); °H_2O.

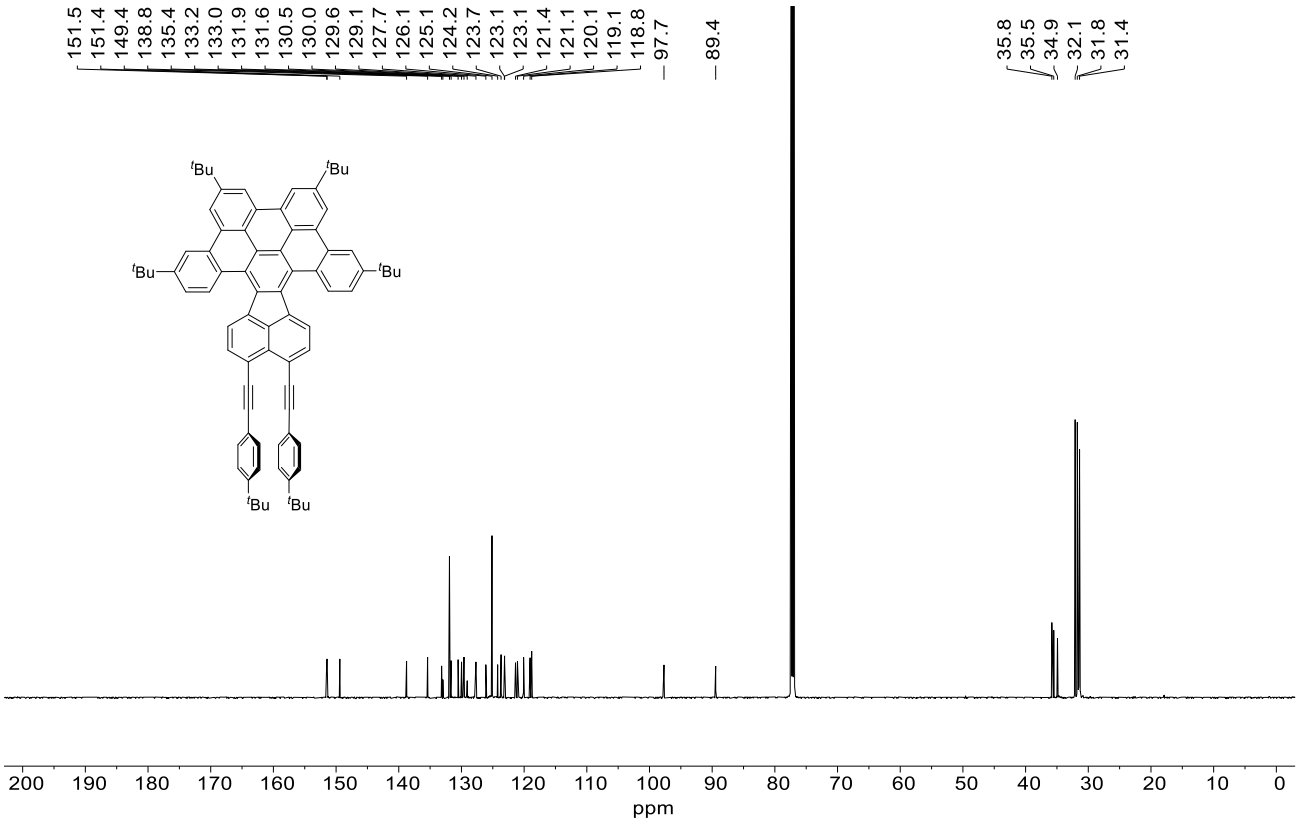

Figure S20: ^{13}C NMR spectrum of **6** ($CDCl_3$, 151 MHz, 50 °C).

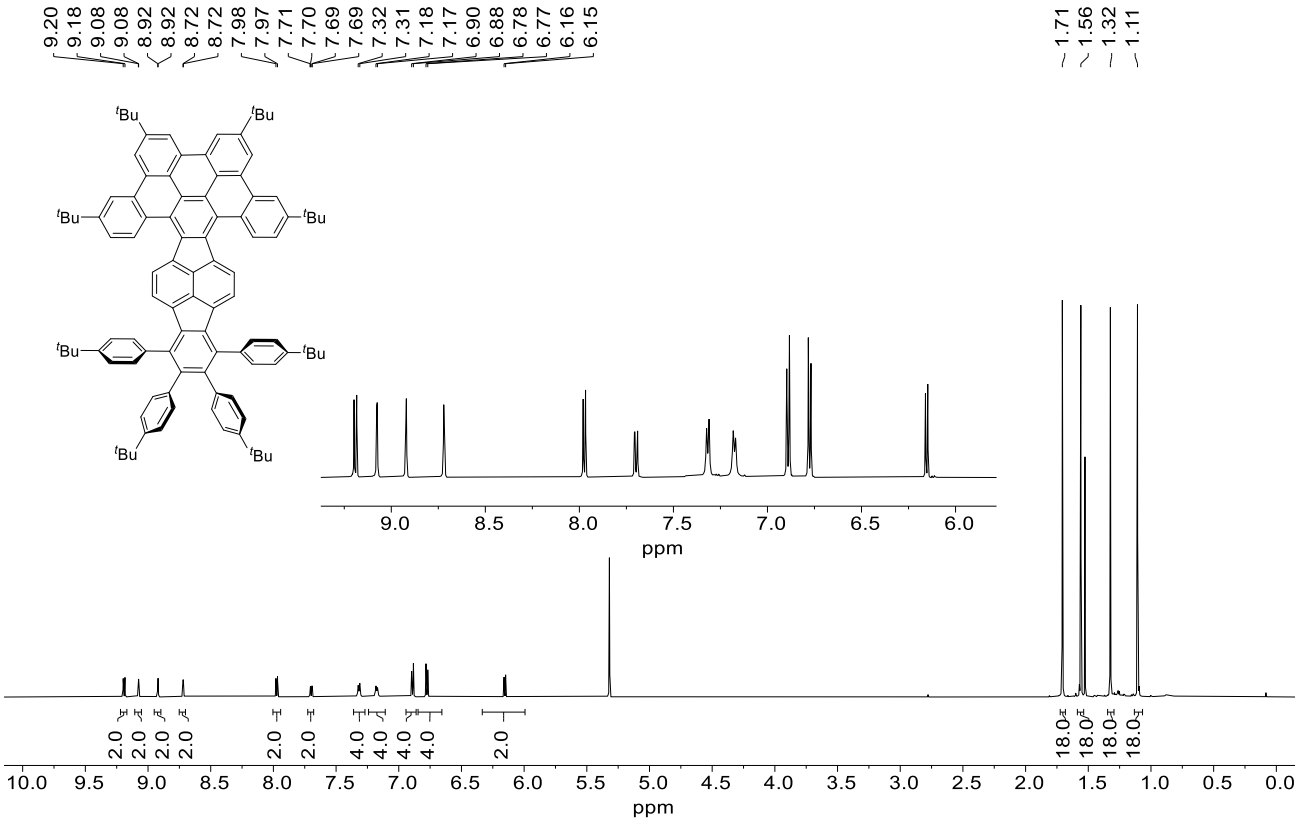

Figure S21: ^{1}H NMR spectrum of **TPP** (CD_2Cl_2, 600 MHz).

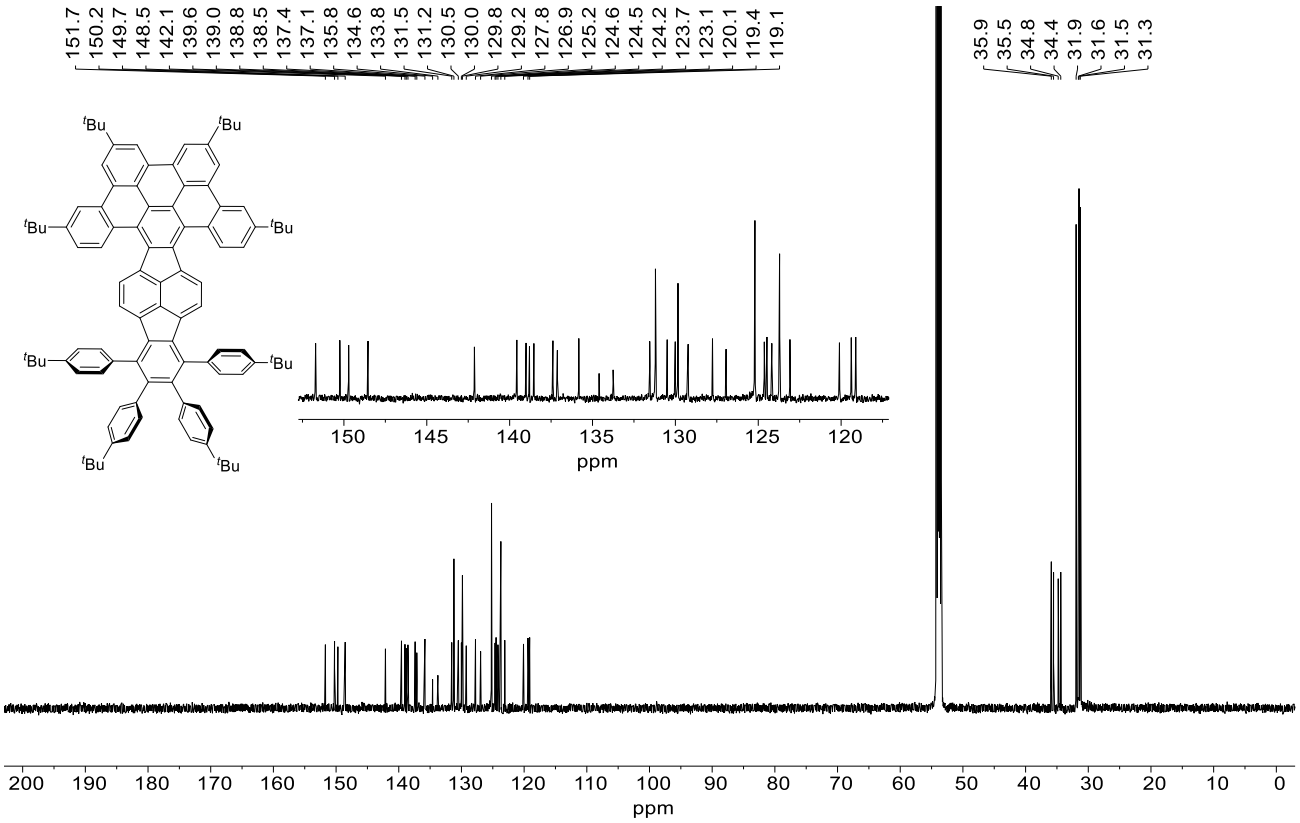

Figure S22: ^{13}C NMR spectrum of **TPP** (CD_2Cl_2, 151 MHz).

4. X-Ray Crystallographic Analysis

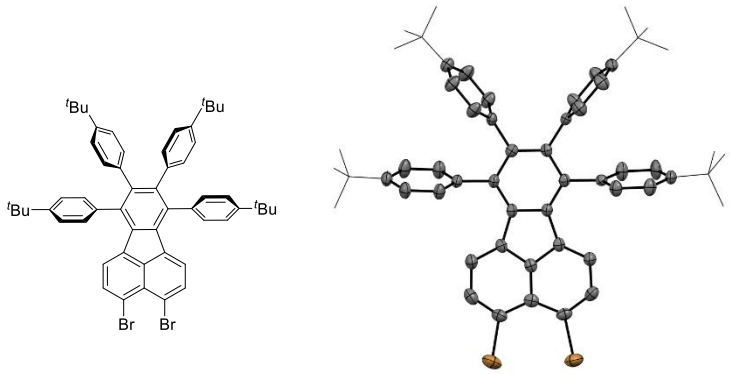

Figure S23: Molecular structure of **3** revealed by X-ray crystallographic analysis.

Single crystals of **3** were obtained by gas phase diffusion of MeOH into a toluene solution of the compound at rt. CCDC 2165129 contains the supplementary crystallographic data for this paper. The data can be obtained free of charge from The Cambridge Crystallographic Data Centre via www.ccdc.cam.ac.uk/structures.

Table S1: Crystal data and structure refinement for **3**.

Empirical Formula		$C_{57}H_{58}Br_2Cl_2$	
Formula Weight		973.75	
Temperature / K		200(2)	
Wavelength / Å		0.71073	
Crystal System		triclinic	
Space Group		P-1	
Z		2	
a / Å	*α* / deg	12.3748(5)	69.3595(9)
b / Å	*β* / deg	14.1094(6)	77.6815(9)
c / Å	*γ* / deg	16.2542(7)	71.9683(9)
Volume / Å^3		2508.01(18)	
Density (Calculated) / g/cm^3		1.29	
Absorption Coefficient / mm^{-1}		1.76	
Crystal Shape (Color)		brick (yellow)	
Crystal Size / mm^3		0.174 × 0.118 × 0.110	
Theta Range for Data Collection / deg		1.3 to 26.0	
Index Ranges		–15≤h≤15, –17≤k≤17, –20≤l≤20	
Reflections Collected		34273	
Reflections (Independent)		9891 (R(int) = 0.0638)	
Reflections (Observed)		5784 (I > 2σ(I))	
Absorption Correction		Semi-empirical from equivalents	
Max. and min. Transmission		0.86 and 0.81	
Refinement Method		Full-matrix least-squares on F^2	
Data/restraints/parameters		9891 / 844 / 594	
Goodness-of-fit on F^2		0.97	
Final R Indices (l > 2σ (l))		R_1 = 0.044, wR_2 = 0.102	
Largest Diff. Peak and Hole / eÅ^{-3}		0.49 and –0.48	

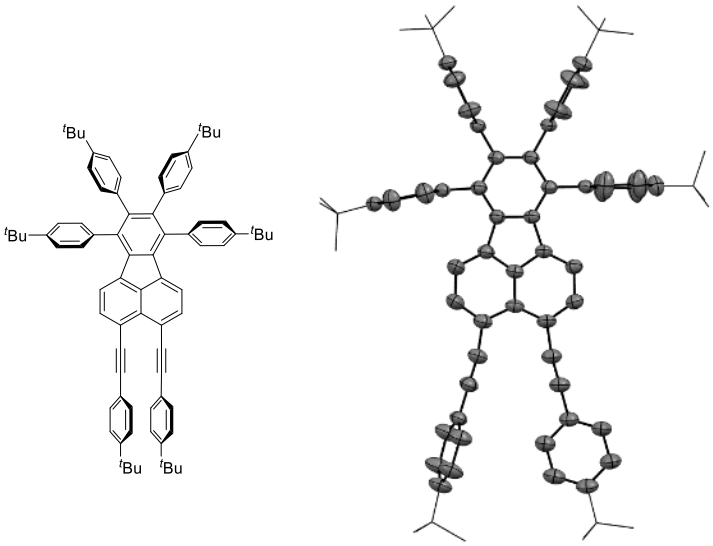

Figure S24: Molecular structure of **4** revealed by X-ray crystallographic analysis.

Single crystals of **4** were obtained by gas phase diffusion of MeOH into a 1,2-dichlorobenzene solution of the compound at rt. CCDC 2165130 contains the supplementary crystallographic data for this paper. The data can be obtained free of charge from The Cambridge Crystallographic Data Centre via www.ccdc.cam.ac.uk/structures.

Table S2: Crystal data and structure refinement for **4**.

Empirical Formula		$C_{80}H_{82}$	
Formula Weight		1043.45	
Temperature / K		200(2)	
Wavelength / Å		1.54178	
Crystal System		monoclinic	
Space Group		$P2_1/m$	
Z		6	
a / Å	α / deg	18.0935(4)	90
b / Å	β / deg	28.7815(5)	106.400(2)
c / Å	γ / deg	23.9554(5)	90
Volume / Å^3		11967.4(4)	
Density (Calculated) / g/cm^3		0.87	
Absorption Coefficient / mm^{-1}		0.36	
Crystal Shape (Color)		plank (yellow)	
Crystal Size / mm^3		0.360 × 0.062 × 0.030	
Theta Range for Data Collection / deg		2.5 to 64.1	
Index Ranges		$-21\leq h\leq 19$, $-17\leq k\leq 33$, $-27\leq l\leq 26$	
Reflections Collected		65402	
Reflections (Independent)		19471 (R(int) = 0.0544)	
Reflections (Observed)		9972 ($l > 2\sigma(l)$)	
Absorption Correction		Semi-empirical from equivalents	
Max. and min. Transmission		0.99 and 0.31	
Refinement Method		Full-matrix least-squares on F^2	
Data/restraints/parameters		19471 / 7388 / 1192	
Goodness-of-fit on F^2		1.05	
Final R Indices ($l > 2\sigma$ (l))		R_1 = 0.105, wR_2 = 0.306	
Largest Diff. Peak and Hole / eÅ^{-3}		0.76 and –0.55	

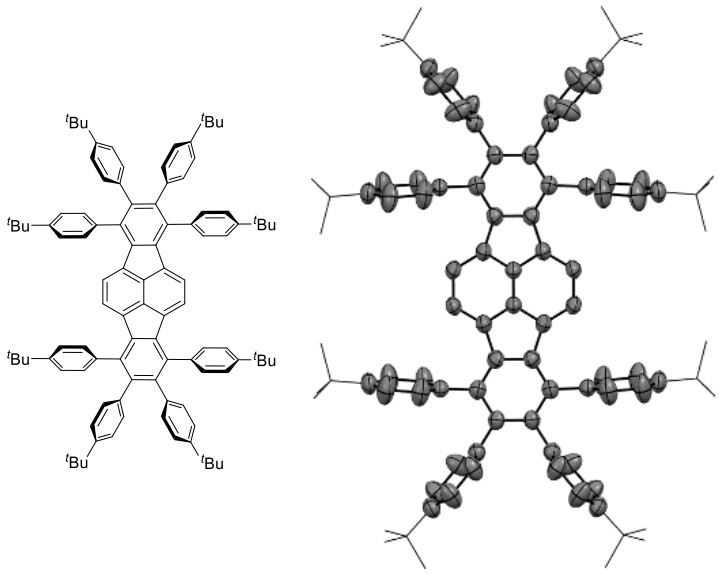

Figure S25: Molecular structure of **OPP** revealed by X-ray crystallographic analysis.

Single crystals of **OPP** were obtained by gas phase diffusion of MeOH into a toluene solution of the compound at rt. CCDC 2165131 contains the supplementary crystallographic data for this paper. The data can be obtained free of charge from The Cambridge Crystallographic Data Centre via www.ccdc.cam.ac.uk/structures.

Table S3: Crystal data and structure refinement for **OPP**.

Empirical Formula		$C_{109}H_{116}$	
Formula Weight		1426.01	
Temperature / K		200(2)	
Wavelength / Å		1.54178	
Crystal System		orthorhombic	
Space Group		*P*nnm	
Z		2	
a / Å	*α* / deg	11.3007(9)	90
b / Å	*β* / deg	11.6891(7)	90
c / Å	*γ* / deg	34.424(2)	90
Volume / Å^3		4547.2(6)	
Density (Calculated) / g/cm^3		1.04	
Absorption Coefficient / mm^{-1}		0.43	
Crystal Shape (Color)		plate (yellow)	
Crystal Size / mm^3		0.050 × 0.037 × 0.026	
Theta Range for Data Collection / deg		4.0 to 47.8	
Index Ranges		$-9\leq h\leq 10$, $-11\leq k\leq 10$, $-29\leq l\leq 33$	
Reflections Collected		9277	
Reflections (Independent)		2161 (R(int) = 0.1208)	
Reflections (Observed)		995 ($l > 2\sigma(l)$)	
Absorption Correction		Semi-empirical from equivalents	
Max. and min. Transmission		0.99 and 0.58	
Refinement Method		Full-matrix least-squares on F^2	
Data/restraints/parameters		2161 / 365 / 245	
Goodness-of-fit on F^2		0.95	
Final R Indices ($l > 2\sigma$ (l))		R_1 = 0.071, wR_2 = 0.165	
Largest Diff. Peak and Hole / eÅ^{-3}		0.25 and –0.20	

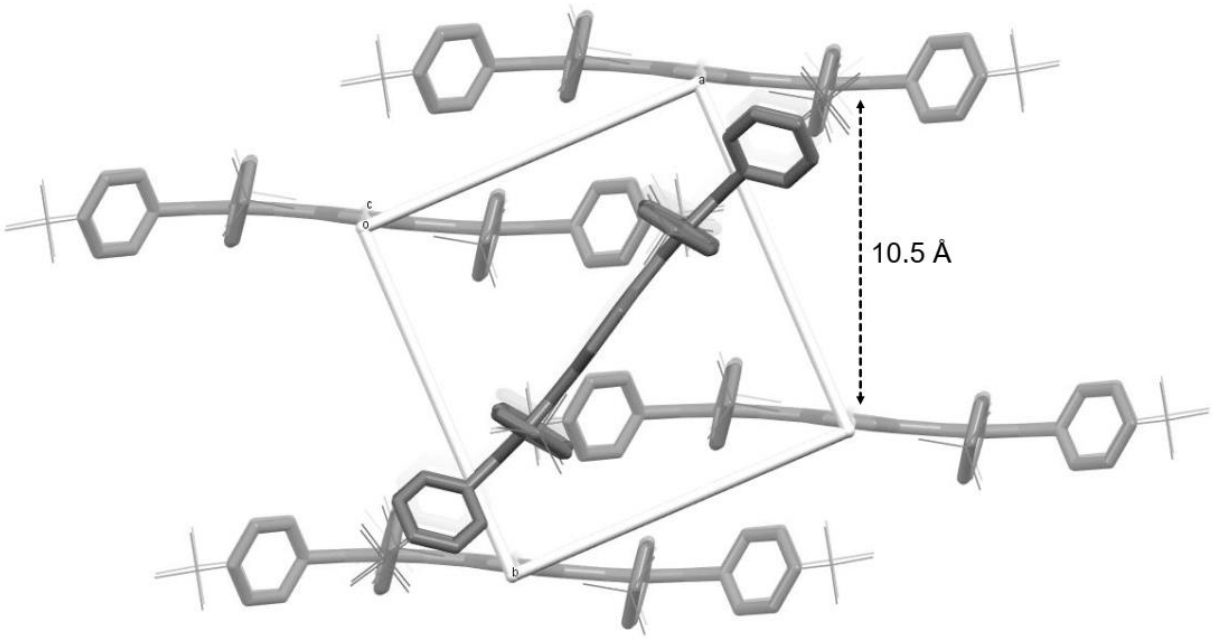

Figure S26: Unit cell of **OPP** along the c axis.

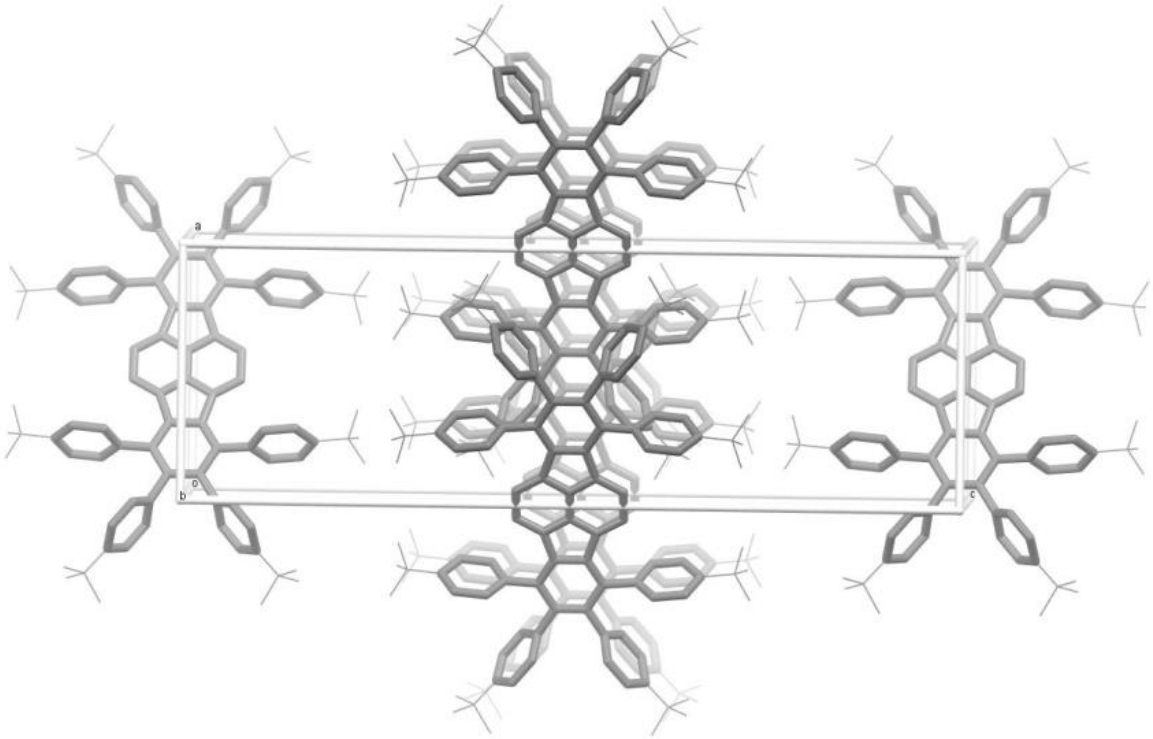

Figure S27: Unit cell of **OPP** along the b axis.

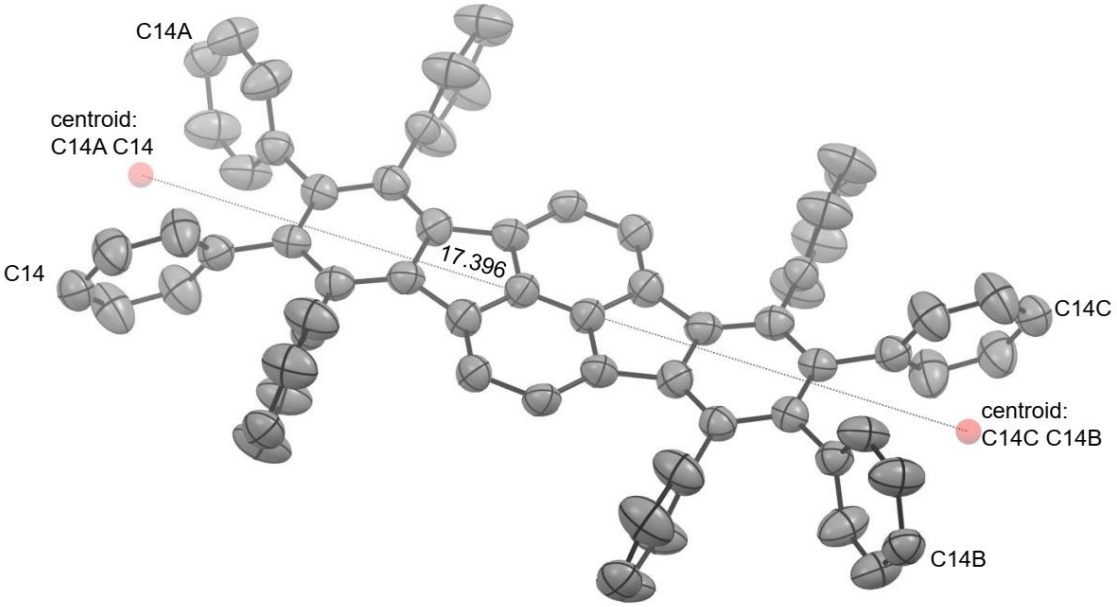

Figure S28: Molecular length of **OPP** (^{t}Bu groups and hydrogens are omitted for clarity).

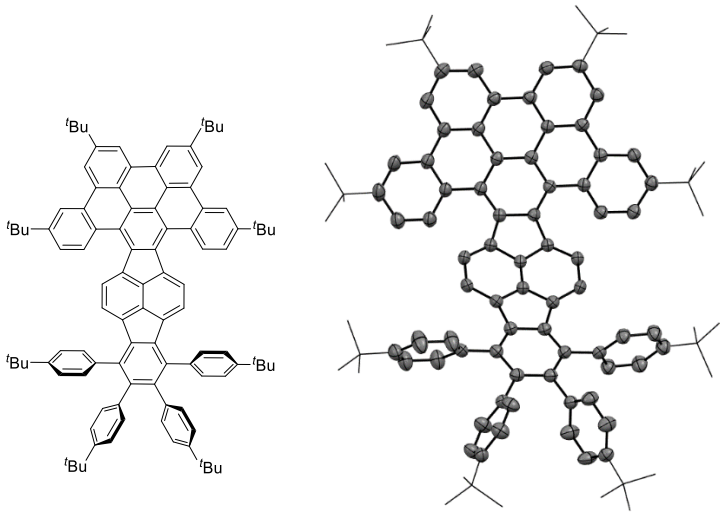

Figure S29: Molecular structure of **TPP** revealed by X-ray crystallographic analysis.

Single crystals of **TPP** were obtained by gas phase diffusion of MeOH into a 1,2-dichlorobenzene solution of the compound at rt. CCDC 2165132 contains the supplementary crystallographic data for this paper. The data can be obtained free of charge from The Cambridge Crystallographic Data Centre via www.ccdc.cam.ac.uk/structures.

Table S4: Crystal data and structure refinement for **TPP**.

Empirical Formula		$C_{123}H_{116}Cl_7$	
Formula Weight		1842.30	
Temperature / K		200(2)	
Wavelength / Å		1.54178	
Crystal System		monoclinic	
Space Group		$P2_1/c$	
Z		4	
a / Å	*α* / deg	19.7230(3)	90
b / Å	*β* / deg	24.5173(4)	106.068(1)
c / Å	*γ* / deg	21.9327(3)	90
Volume / Å^3		10191.3(3)	
Density (Calculated) / g/cm^3		1.20	
Absorption Coefficient / mm^{-1}		2.15	
Crystal Shape (Color)		brick (red)	
Crystal Size / mm^3		0.176 × 0.162 × 0.093	
Theta Range for Data Collection / deg		2.3 to 69.4	
Index Ranges		$-18\leq h\leq 23$, $-29\leq k\leq 28$, $-22\leq l\leq 26$	
Reflections Collected		67693	
Reflections (Independent)		18512 (R(int) = 0.0336)	
Reflections (Observed)		12142 ($I > 2\sigma(I)$)	
Absorption Correction		Semi-empirical from equivalents	
Max. and min. Transmission		0.97 and 0.55	
Refinement Method		Full-matrix least-squares on F^2	
Data/restraints/parameters		18512 / 1910 / 1293	
Goodness-of-fit on F^2		1.03	
Final R Indices ($I > 2\sigma(I)$)		R_1 = 0.063, wR_2 = 0.175	
Largest Diff. Peak and Hole / eÅ^{-3}		0.66 and –0.68	

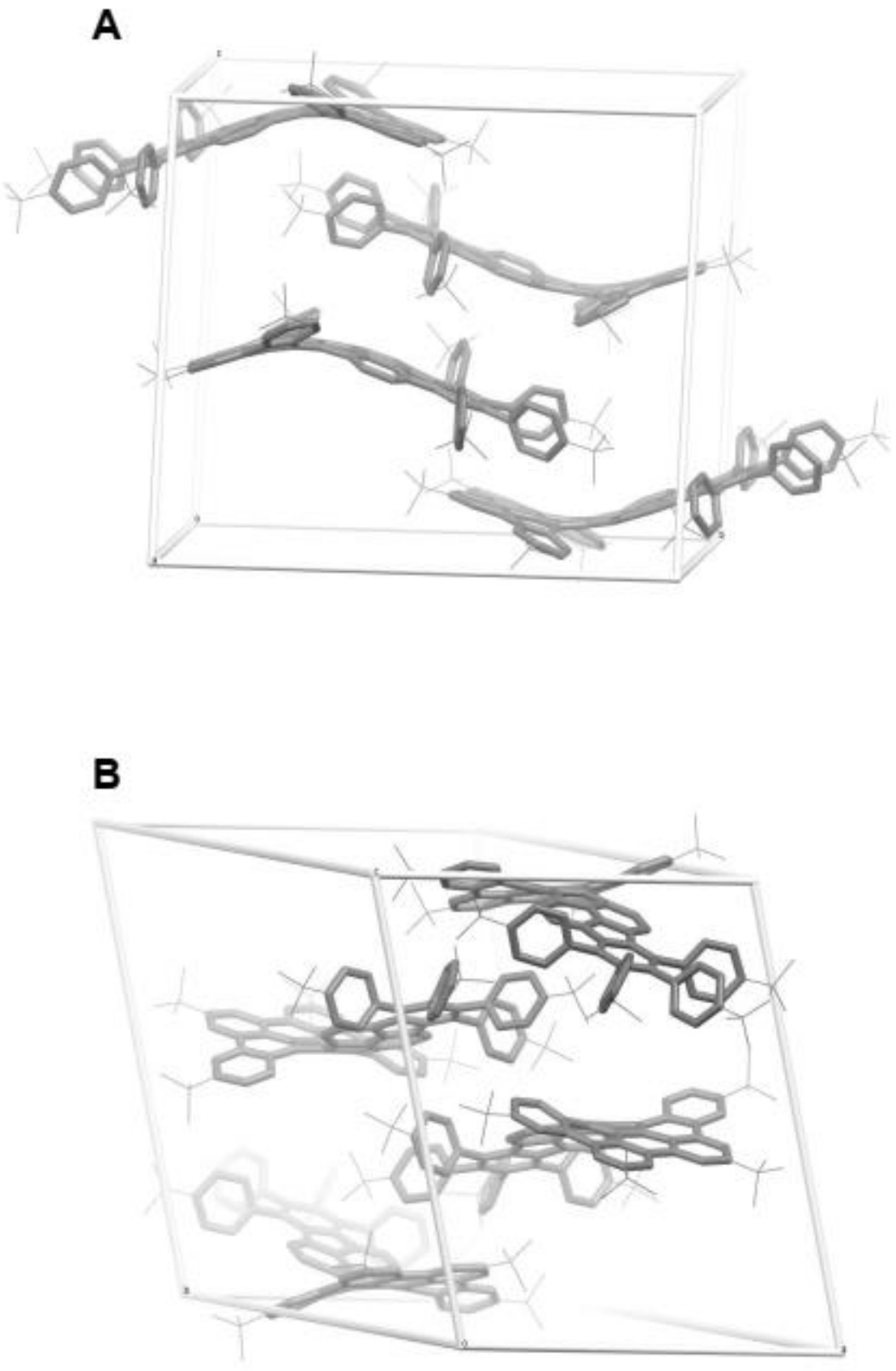

Figure S30: **A**: Unit cell of **TPP** along the a axis. **B**: Unit cell of **TPP** along the ab axis.

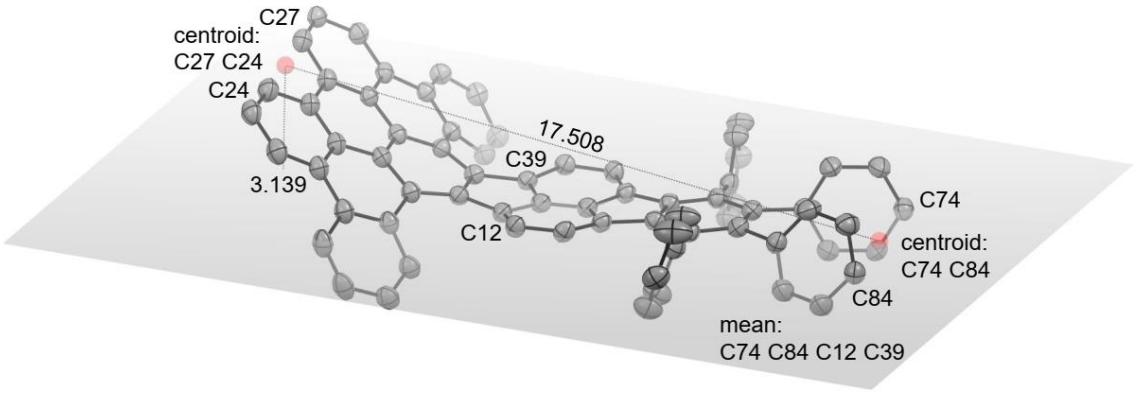

Figure S31: Molecular length and depth of **TPP** (ᵗBu groups and hydrogens are omitted for clarity).

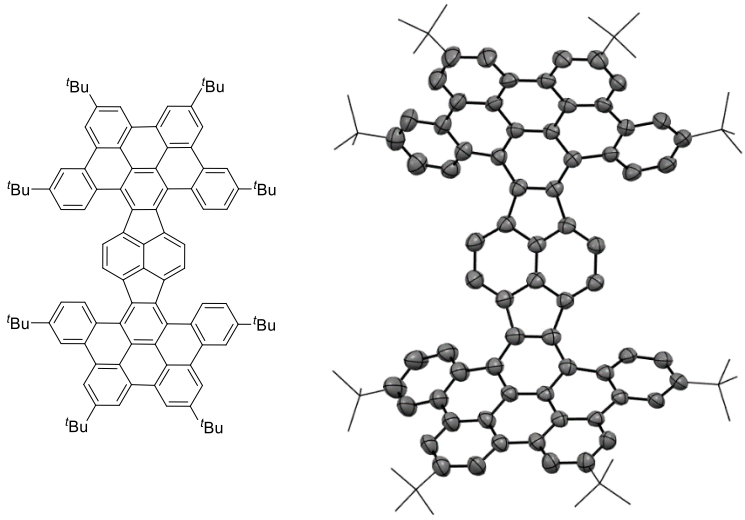

Figure S32: Molecular structure of **HPH** revealed by X-ray crystallographic analysis.

Single crystals of **HPH** were obtained by gas phase diffusion of MeOH into a 1,2-dichlorobenzene solution of the compound at rt. CCDC 2165133 contains the supplementary crystallographic data for this paper. The data can be obtained free of charge from The Cambridge Crystallographic Data Centre via www.ccdc.cam.ac.uk/structures.

Table S5: Crystal data and structure refinement for **HPH**.

Empirical Formula		$C_{108}H_{100}Cl_2$	
Formula Weight		1468.77	
Temperature / K		200(2)	
Wavelength / Å		0.71073	
Crystal System		monoclinic	
Space Group		*C*2/c	
Z		8	
a / Å	*α* / deg	36.177(2)	90
b / Å	*β* / deg	21.9801(12)	94.4606(14)
c / Å	*γ* / deg	25.6958(15)	90
Volume / Å^3		20371(2)	
Density (Calculated) / g/cm^3		0.96	
Absorption Coefficient / mm^{-1}		0.10	
Crystal Shape (Color)		plank (violet)	
Crystal Size / mm^3		0.600 × 0.091 × 0.034	
Theta Range for Data Collection / deg		1.1 to 19.4	
Index Ranges		–33≤h≤33, –20≤k≤20, –24≤l≤24	
Reflections Collected		62342	
Reflections (Independent)		8739 (R(int) = 0.0752)	
Reflections (Observed)		5543 (l > 2σ(l))	
Absorption Correction		Semi-empirical from equivalents	
Max. and min. Transmission		0.96 and 0.72	
Refinement Method		Full-matrix least-squares on F^2	
Data/restraints/parameters		8739 / 1822 / 991	
Goodness-of-fit on F^2		1.03	
Final R Indices (l > 2σ (l))		R_1 = 0.107, wR_2 = 0.296	
Largest Diff. Peak and Hole / eÅ^{-3}		1.60 and –0.39	

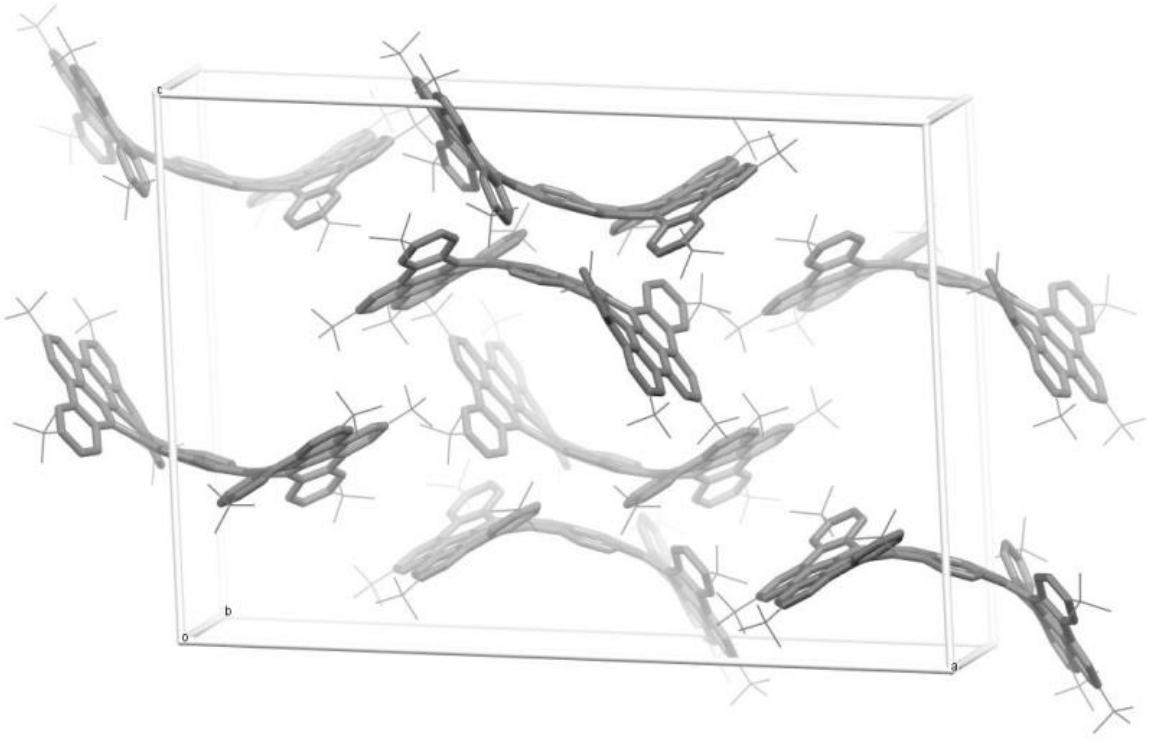

Figure S33: Unit cell of **HPH** along the b axis. Molecules are shown as capped sticks model and ^{t}Bu groups as wireframe.

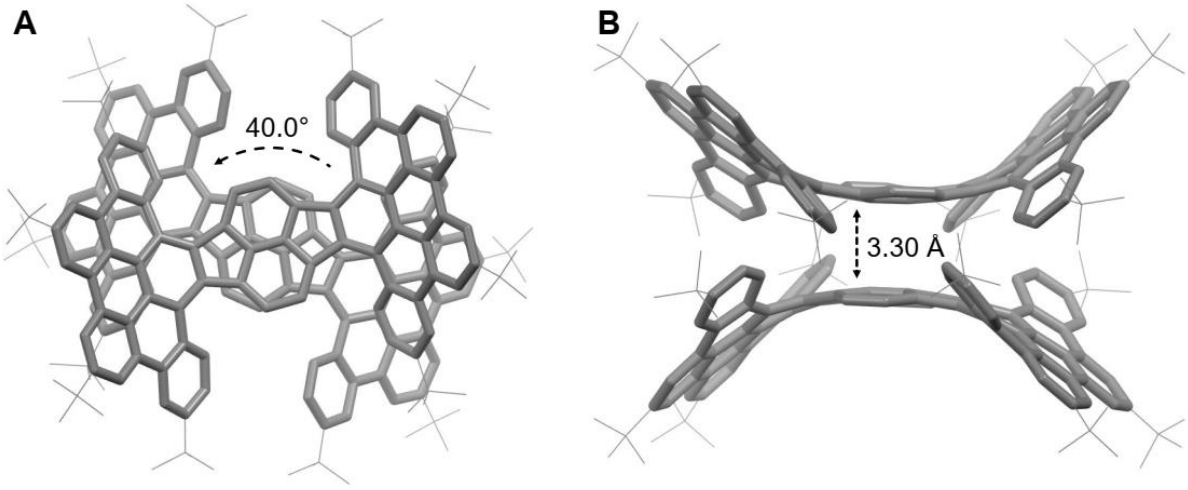

Figure S34: Capped sticks model of **HPH**. **A**: Adjacent molecules are twisted. **B**: Interacting molecules in close proximity.

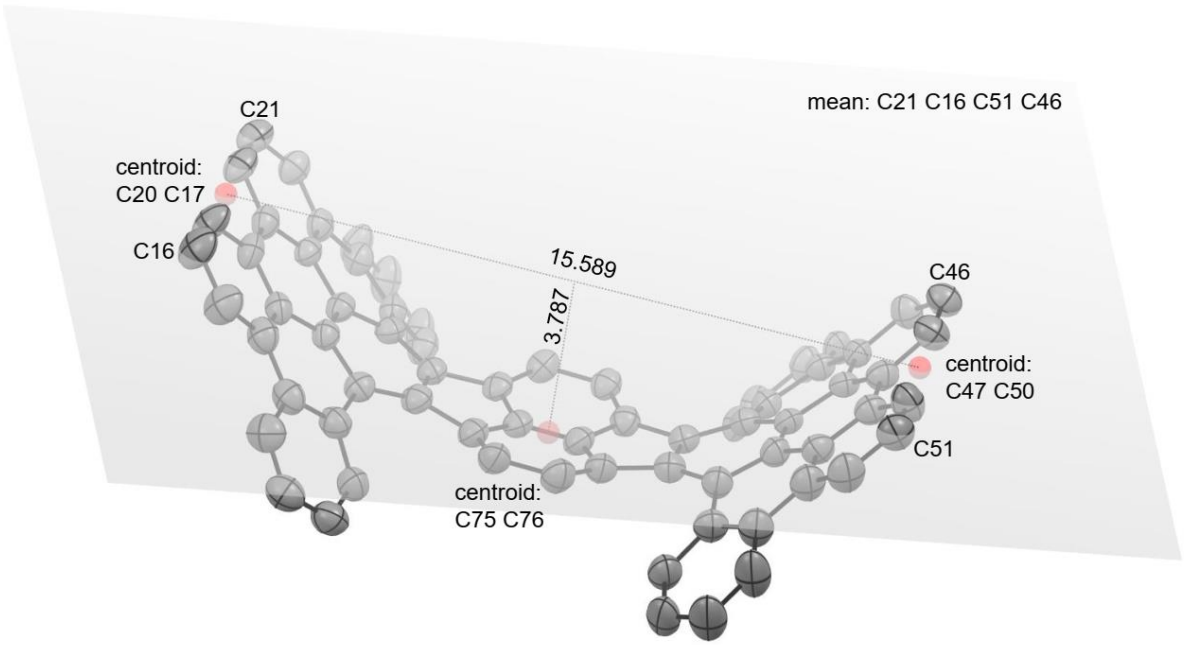

Figure S35: Determination of the bowl depth in **HPH-boat** (ᵗBu groups and hydrogens are omitted for clarity).

5. UV/vis Absorption and Emission Spectroscopy Data

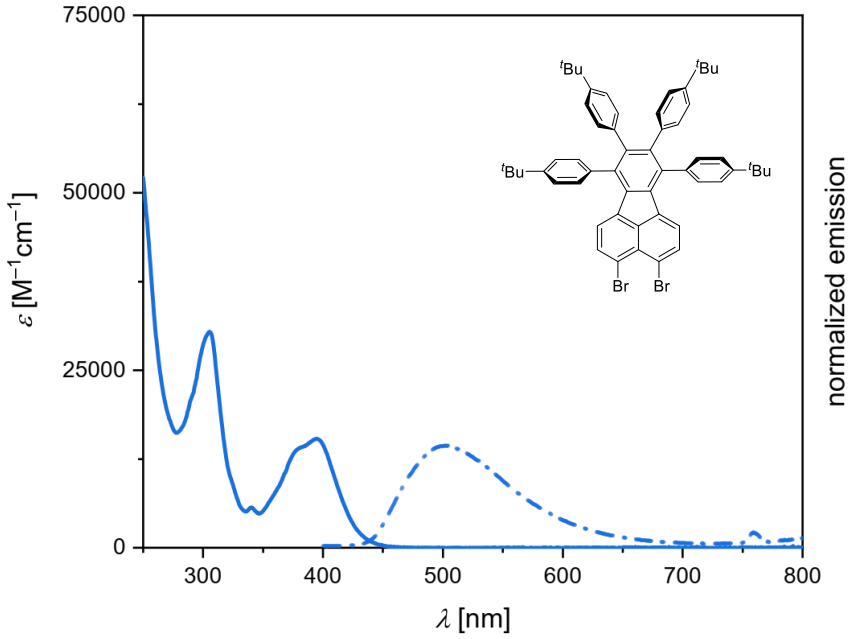

Figure S36: UV/vis absorption and emission spectra (normalized) of compound **3** in CH_2Cl_2.

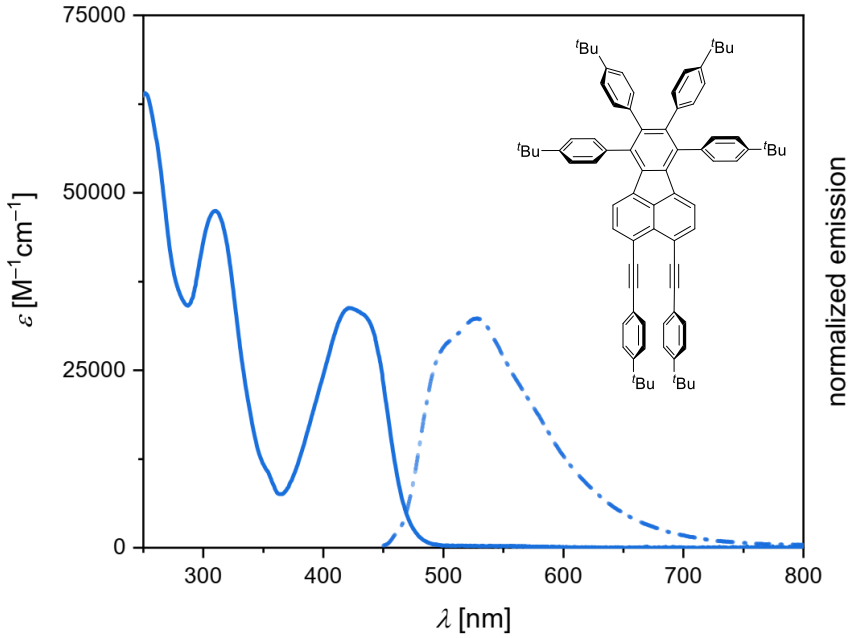

Figure S37: UV/vis absorption and emission spectra (normalized) of compound **4** in CH_2Cl_2.

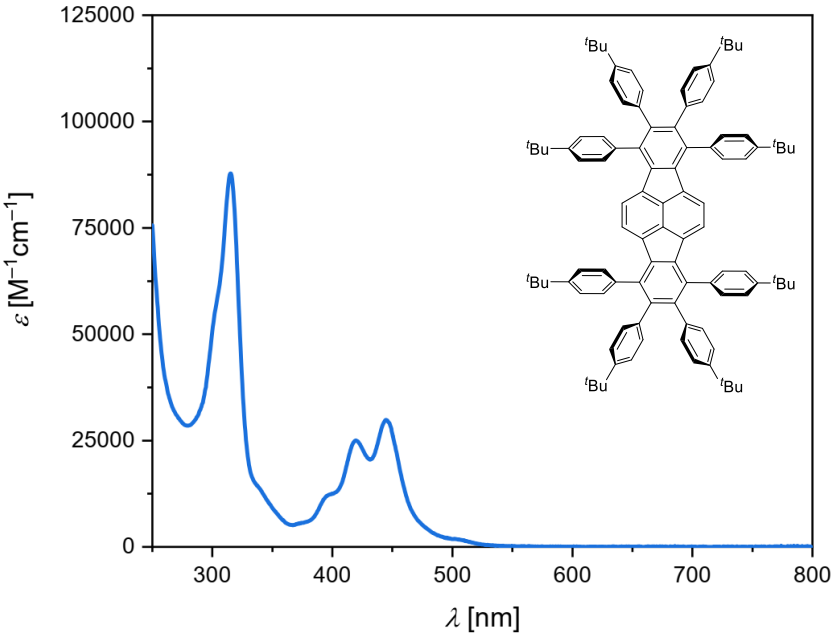

Figure S38: UV/vis absorption of compound **OPP** in CH_2Cl_2.

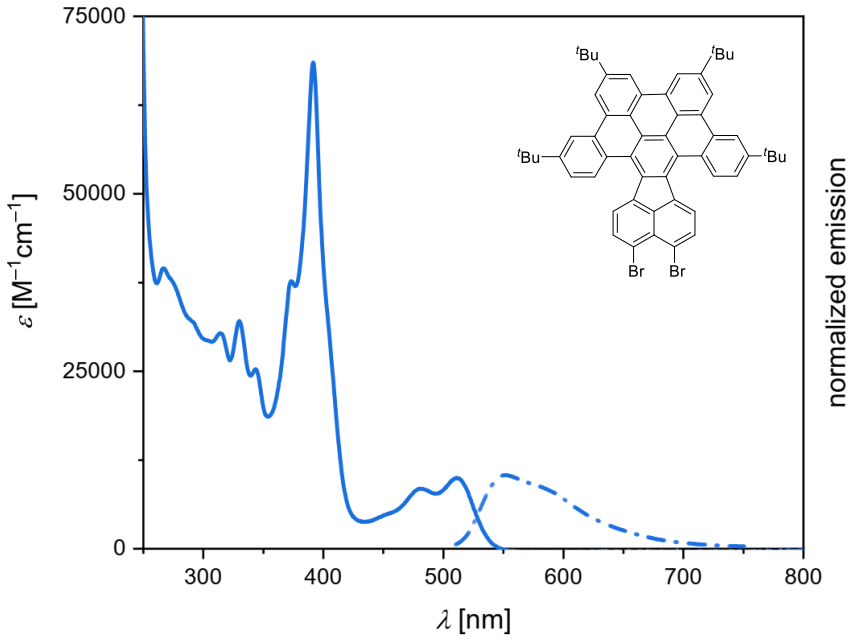

Figure S39: UV/vis absorption and emission spectra (normalized) of compound **5** in CH_2Cl_2.

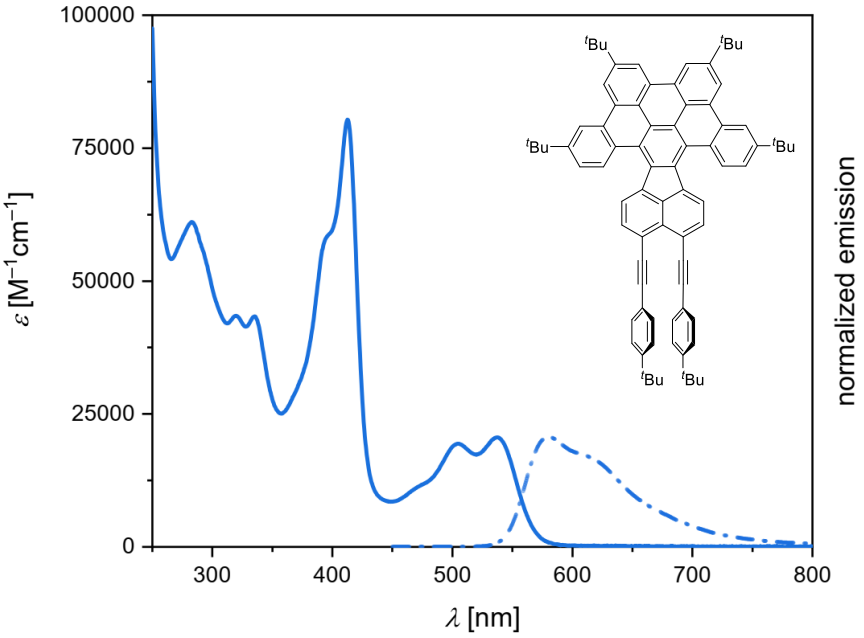

Figure S40: UV/vis absorption and emission spectra (normalized) of compound **6** in CH_2Cl_2.

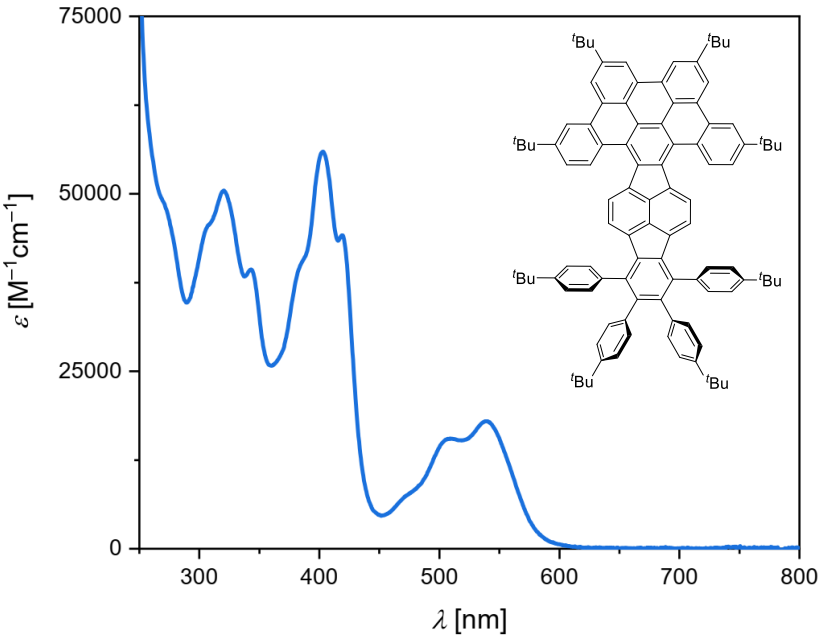

Figure S41: UV/vis absorption spectrum of compound **TPP** in CH_2Cl_2.

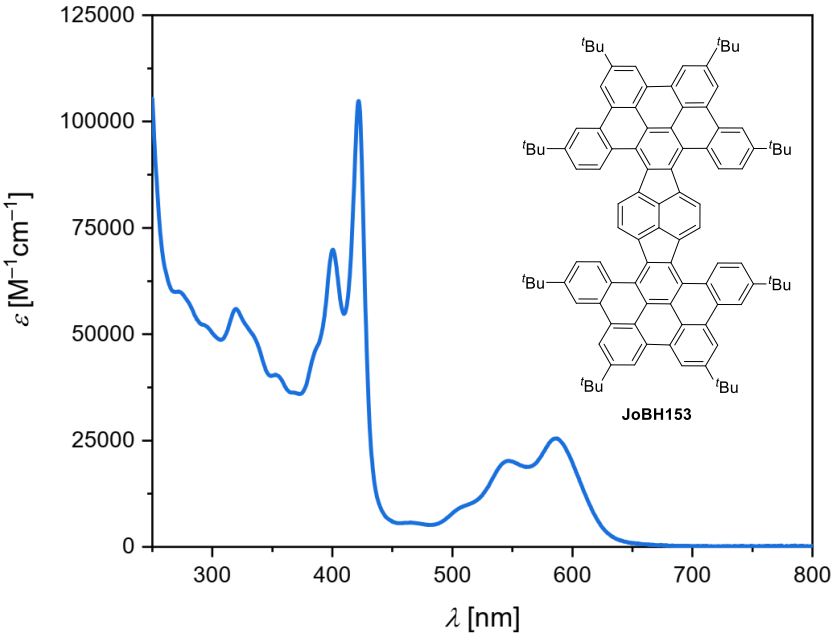

Figure S42: UV/vis absorption spectrum of compound **HPH** in CH_2Cl_2.

6. Cyclic Voltammetry Data

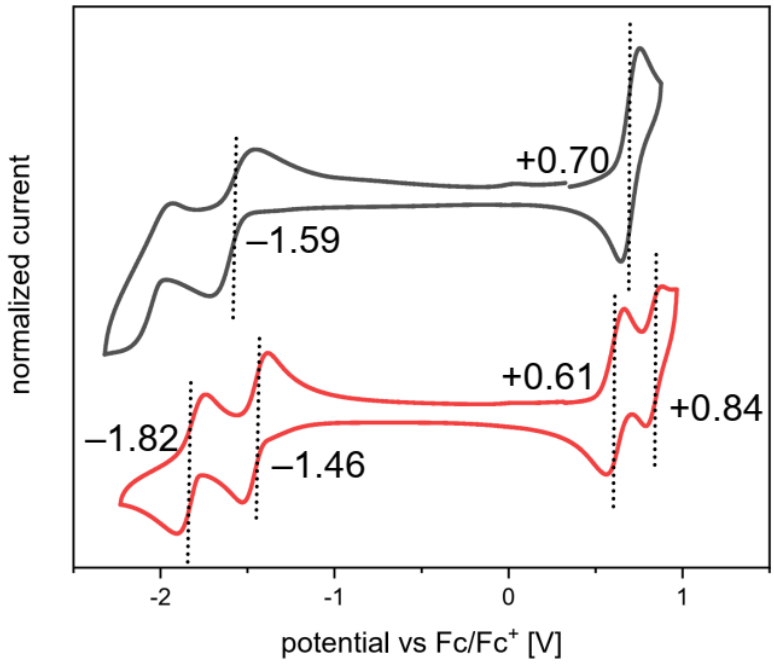

Figure S43: CV data of **TPP** (red) and **HPH** (violet) measured in CH_2Cl_2 at rt and referenced to Fc/Fc^+ (scan rate 149 mV sec^{-1}).

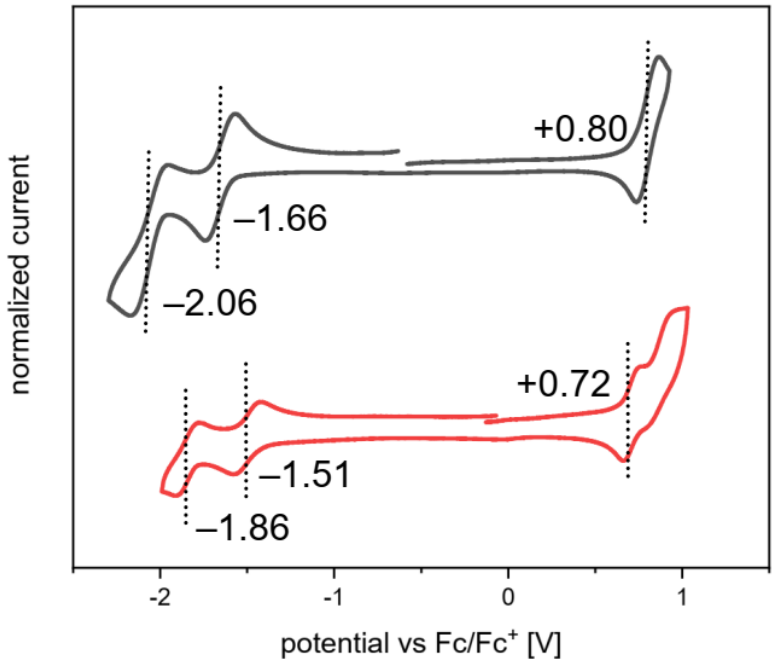

Figure S44: CV data of **TPP** (red) and **HPH** (violet) measured in THF at rt and referenced to Fc/Fc^+ (scan rate 149 mV sec^{-1}).

7. Theoretical Absorption Spectra

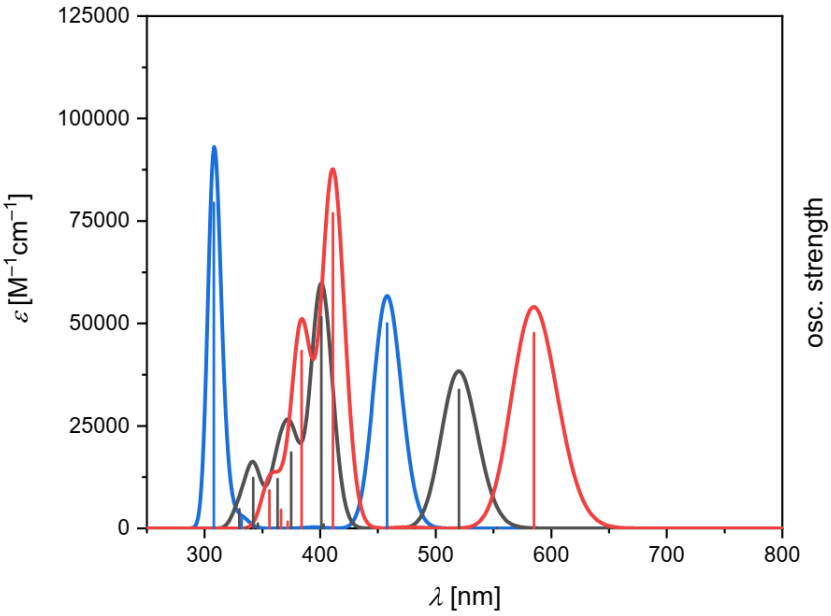

Figure S45: Theoretical UV/vis spectra TD-DFT (CAM-B3LYP/6-31G(d)) of **OPP** (blue), **TPP** (black), **HPH** (red).

Table S6:Vertical excitations of **OPP** calculated at TD CAM-B3LYP/6-31G(d) in vacuum. Only the orbital contributions with the largest expansion coefficient (in parentheses) are shown.

Excitation	***E* [eV]**	**λ [nm]**	**Type**	***f***
S_1	3.09	402	HOMO → LUMO (0.98)	0.00
S_2	3.48	356	HOMO → LUMO (0.95)	1.00
S_3	3.91	318	HOMO–6 → LUMO (0.80)	0.00
S_4	4.24	292	HOMO–1 → LUMO (0.75)	0.00
S_5	4.50	276	HOMO–2 → LUMO (0.87)	0.05
S_6	4.64	267	HOMO–4 → LUMO (0.65)	0.18
S_7	4.68	265	HOMO–3 → LUMO (0.57)	0.00
S_8	4.68	265	HOMO–3 → LUMO (0.65)	0.01
S_9	4.71	263	HOMO–1 → LUMO (0.61)	0.00
S_{10}	4.79	259	HOMO → LUMO+1 (0.79)	1.59

Table S7:Vertical excitations of **TPP** calculated at TD CAM-B3LYP/6-31G(d) in vacuum. Only the orbital contributions with the largest expansion coefficient (in parentheses) are shown.

Excitation	***E* [eV]**	**λ [nm]**	**Type**	***f***
S_1	2.81	442	HOMO–1 → LUMO (0.92)	0.00
S_2	2.94	422	HOMO → LUMO (0.91)	0.68
S_3	3.64	341	HOMO–3 → LUMO (0.60)	0.02
S_4	3.65	340	HOMO–1 → LUMO+1 (0.62)	1.03
S_5	3.86	321	HOMO → LUMO+1 (0.79)	0.37
S_6	3.98	312	HOMO–2 → LUMO (0.62)	0.24
S_7	4.14	299	HOMO–4 → LUMO (0.77)	0.02
S_8	4.19	296	HOMO–3 → LUMO (0.43)	0.25
S_9	4.25	292	HOMO–5 → LUMO (0.80)	0.00
S_{10}	4.31	288	HOMO → LUMO+2 (0.68)	0.09

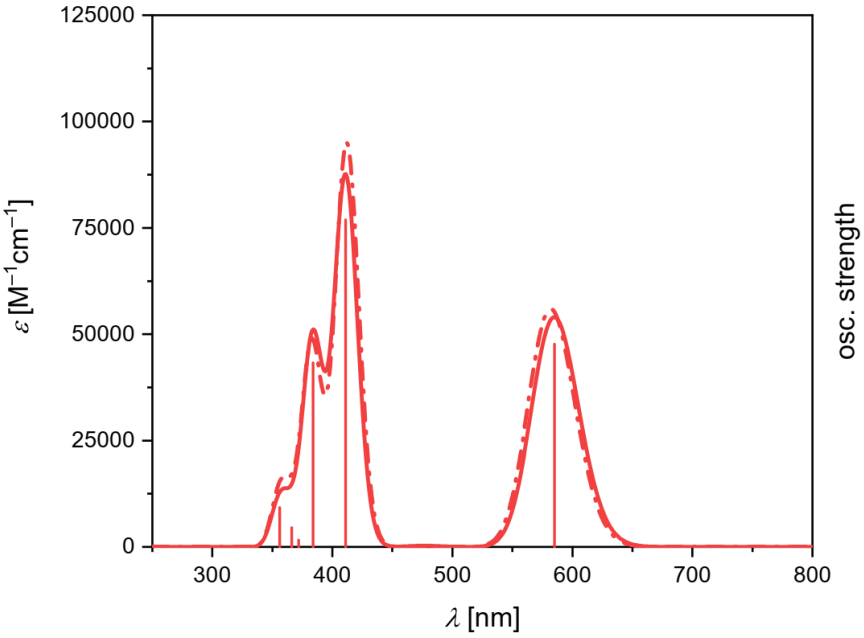

Figure S46: Theoretical UV/vis spectra (CAM-B3LYP/6-31G(d)) of **HPH-boat** (full line) and **HPH-chair** (dashed line).

Table S8:Vertical excitations of **OPP-boat** calculated at TD CAM-B3LYP/6-31G(d) in vacuum. Only the orbital contributions with the largest expansion coefficient (in parentheses) are shown.

Excitation	***E* [eV]**	**λ [nm]**	**Type**	***f***
S_1	2.64	469	HOMO–1 → LUMO (0.94)	0.00
S_2	2.74	452	HOMO → LUMO (0.94)	0.95
S_3	3.22	385	HOMO–2 → LUMO (0.80)	0.00
S_4	3.40	365	HOMO–3 → LUMO (0.78)	0.00
S_5	3.64	341	HOMO–1 → LUMO+1 (0.77)	1.54
S_6	3.74	332	HOMO → LUMO+1 (0.81)	0.00
S_7	3.85	322	HOMO → LUMO+2 (0.68)	0.87
S_8	3.96	313	HOMO–1 → LUMO+2 (0.52)	0.03
S_9	4.01	310	HOMO–4 → LUMO (0.85)	0.09
S_{10}	4.09	303	HOMO–11 → LUMO (0.61)	0.18

Table S9:Vertical excitations of **OPP-chair** calculated at TD CAM-B3LYP/6-31G(d) in vacuum. Only the orbital contributions with the largest expansion coefficient (in parentheses) are shown.

Excitation	***E* [eV]**	**λ [nm]**	**Type**	***f***
S_1	2.65	468	HOMO–1 → LUMO (0.93)	0.00
S_2	2.75	451	HOMO → LUMO (0.94)	0.99
S_3	3.22	384	HOMO–2 → LUMO (0.80)	0.00
S_4	3.40	365	HOMO–3 → LUMO (0.78)	0.00
S_5	3.63	341	HOMO–1 → LUMO+1 (0.77)	1.67
S_6	3.74	332	HOMO → LUMO+1 (0.81)	0.00
S_7	3.86	321	HOMO → LUMO+2 (0.67)	0.84
S_8	3.96	313	HOMO–2 → LUMO+2 (0.52)	0.00
S_9	4.02	308	HOMO–4 → LUMO (0.82)	0.13
S_{10}	4.10	302	HOMO–11 → LUMO (0.60)	0.21

8. Ground State Energy

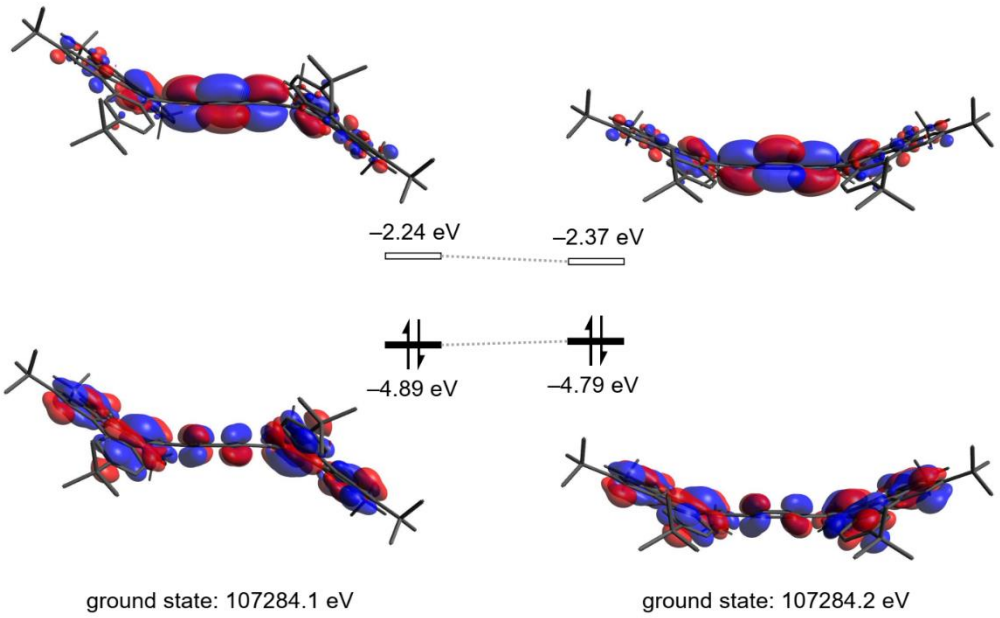

Figure S47: Calculated ground state energies (CAM-B3LYP/6-31G(d)) and HOMO/LUMO energies (B3LYP/6-31G(d)) of the chair-shaped conformer (left) and boat-shaped conformer (right) of **HPH**.

9. Nucleus Independent Chemical Shift (NICS)

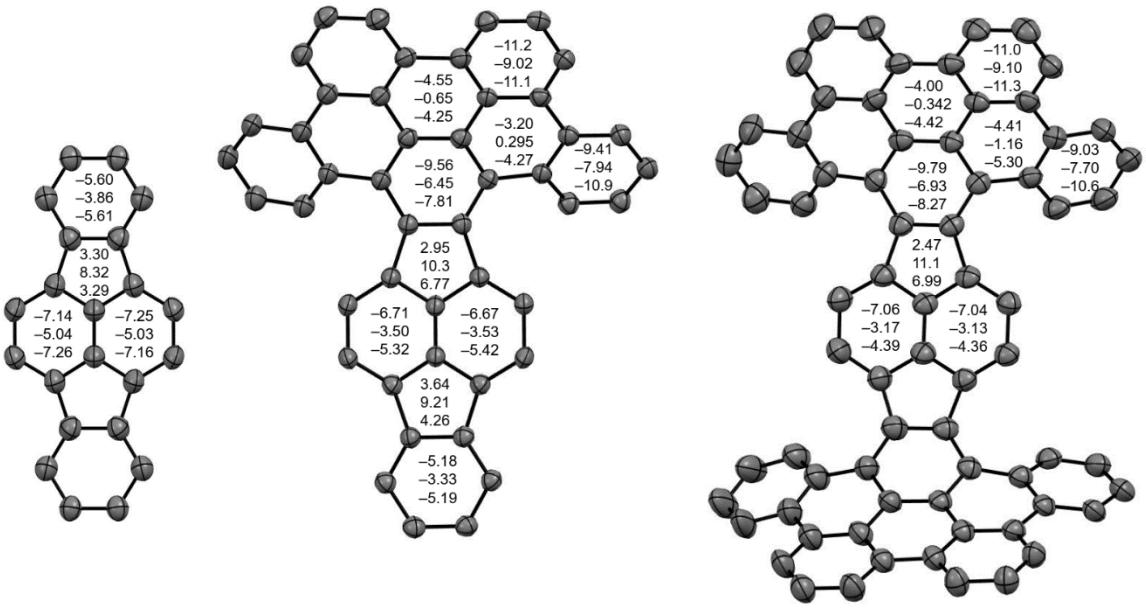

Figure S48: NICS(+1/0/–1) values for compounds **OPP**, **TPP** and **HPH**. Top: NICS(+1), Center: NICS(0); Bottom: NICS(–1).

10. Harmonic Oscillator Model of Aromaticity (HOMA)

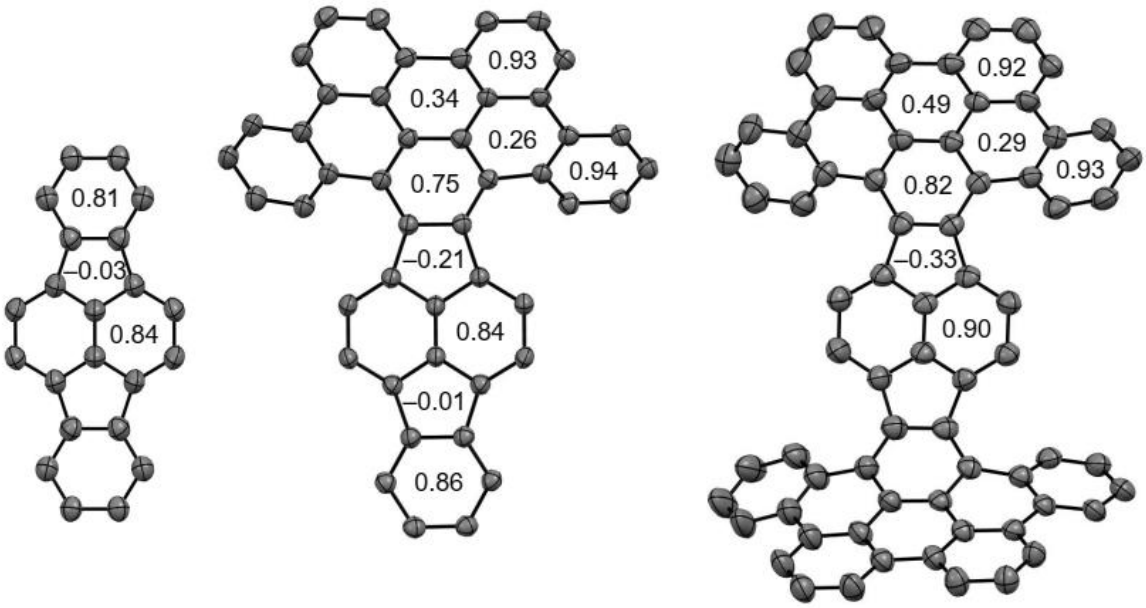

Figure S49: HOMA values for compounds **OPP**, **TPP** and **HPH**.

11. Pyramidalization of Atomic Vectors (POAV)

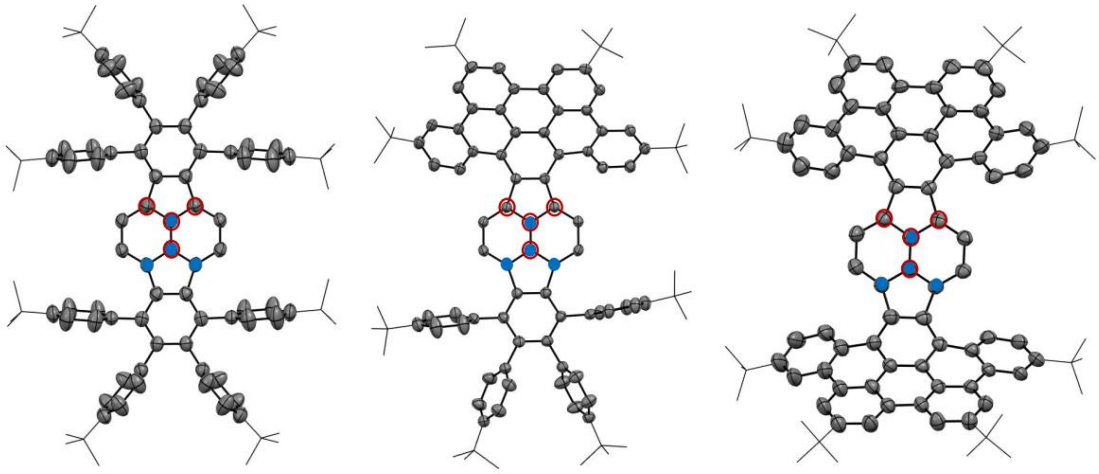

POAV	**OPP**	**TPP**	**HPH**
Top	0.04°	2.04°	2.10°
Bottom	0.04°	1.37°	2.10°

Figure S50: Estimated POAV values for compounds **OPP**, **TPP** and **HPH**.

12. References

[1] G. R. Fulmer, A. J. M. Miller, N. H. Sherden, H. E. Gottlieb, A. Nudelman, B. M. Stoltz, J. E. Bercaw, K. I. Goldberg, *Organometallics* **2010**, *29*, 2176.

[2] G. M. Sheldrick, *Acta Crystallogr. A* **2008**, *64*, 112.

[3] G. M. Sheldrick, *Acta Crystallogr. C* **2015**, *71*, 3.

[4] C. F. Macrae, P. R. Edgington, P. McCabe, E. Pidcock, G. P. Shields, R. Taylor, M. Towler, J. van de Streek, *J. Appl. Cryst.* **2006**, *39*, 453.

[5] Gaussian 16, Revision B.01, M. J. Frisch, G. W. Trucks, H. B. Schlegel, G. E. Scuseria, M. A. Robb, J. R. Cheeseman, G. Scalmani, V. Barone, G. A. Petersson, H. Nakatsuji, X. Li, M. Caricato, A. V. Marenich, J. Bloino, B. G. Janesko, R. Gomperts, B. Mennucci, H. P. Hratchian, J. V. Ortiz, A. F. Izmaylov, J. L. Sonnenberg, D. Williams-Young, F. Ding, F. Lipparini, F. Egidi, J. Goings, B. Peng, A. Petrone, T. Henderson, D. Ranasinghe, V. G. Zakrzewski, J. Gao, N. Rega, G. Zheng, W. Liang, M. Hada, M. Ehara, K. Toyota, R. Fukuda, J. Hasegawa, M. Ishida, T. Nakajima, Y. Honda, O. Kitao, H. Nakai, T. Vreven, K. Throssell, J. A. Montgomery, Jr., J. E. Peralta, F. Ogliaro, M. J. Bearpark, J. J. Heyd, E. N. Brothers, K. N. Kudin, V. N. Staroverov, T. A. Keith, R. Kobayashi, J. Normand, K. Raghavachari, A. P. Rendell, J. C. Burant, S. S. Iyengar, J. Tomasi, M. Cossi, J. M. Millam, M. Klene, C. Adamo, R. Cammi, J. W. Ochterski, R. L. Martin, K. Morokuma, O. Farkas, J. B. Foresman, and D. J. Fox, Gaussian, Inc., Wallingford CT, **2016**.

[6] E. Epifanovsky, A. T. B. Gilbert, X. Feng, J. Lee, Yuezhi Mao, N. Mardirossian, P. Pokhilko, A. F. White, M. P. Coons, A. L. Dempwolff, Z. Gan, D. Hait, P. R. Horn, L. D. Jacobson, I. Kaliman, J. Kussmann, Adrian W. Lange, K. U. Lao, D. S. Levine, J. Liu, S. C. McKenzie, A. F. Morrison, K. D. Nanda, F. Plasser, D. R. Rehn, M. L. Vidal, Z.-Q. You, Y. Zhu, B. Alam, B. J. Albrecht, A. Aldossary, E. Alguire, J. H. Andersen, V. Athavale, D. Barton, K. Begam, A. Behn, N. Bellonzi, Y. A. Bernard, E. J. Berquist, H. G. A. Burton, A. Carreras, K. Carter-Fenk, R. Chakraborty, A. D. Chien, K. D. Closser, V. Cofer-Shabica, S. Dasgupta, M. de Wergifosse, J. Deng, M. Diedenhofen, H. Do, S. Ehlert, P.-T. Fang, S. Fatehi, Q. Feng, T. Friedhoff, J. Gayvert, Q. Ge, G. Gidofalvi, M. Goldey, J. Gomes, C. E. González-Espinoza, S. Gulania, A. O. Gunina, M. W. D. Hanson-Heine, P. H. P. Harbach, A. Hauser, M. F. Herbst, M. H. Vera, M. Hodecker, Z. C. Holden, S. Houck, X. Huang, K. Hui, B. C. Huynh, M. Ivanov, Á. Jász, H. Ji, H. Jiang, B. Kaduk, S. Kähler, K. Khistyaev, J. Kim, G. Kis, P. Klunzinger, Z. Koczor-Benda, J. H. Koh, D. Kosenkov, L. Koulias, T. Kowalczyk, C. M. Krauter, K. Kue, A. Kunitsa, T. Kus, I. Ladjánszki, A. Landau, K. V.

Lawler, D. Lefrancois, S. Lehtola, R. R. Li, Y.-P. Li, J. Liang, M. Liebenthal, H.-H. Lin, Y.-S. Lin, F. Liu, K.-Y. Liu, M. Loipersberger, A. Luenser, A. Manjanath, P. Manohar, E. Mansoor, S. F. Manzer, S.-P. Mao, A. V. Marenich, T. Markovich, S. Mason, S. A. Maurer, P. F. McLaughlin, M. F. S. J. Menger, J.-M. Mewes, S. A. Mewes, P. Morgante, J. W. Mullinax, K. J. Oosterbaan, G. Paran, A. C. Paul, S. K. Paul, F. Pavošević, Z. Pei, S. Prager, E. I. Proynov, Á. Rák, E. Ramos-Cordoba, B. Rana, A. E. Rask, A. Rettig, R. M. Richard, F. Rob, E. Rossomme, T. Scheele, M. Scheurer, M. Schneider, N. Sergueev, S. M. Sharada, W. Skomorowski, D. W. Small, C. J. Stein, Y.-C. Su, E. J. Sundstrom, Z. Tao, J. Thirman, G. J. Tornai, T. Tsuchimochi, N. M. Tubman, S. P. Veccham, O. Vydrov, J. Wenzel, J. Witte, A. Yamada, K. Yao, S. Yeganeh, S. R. Yost, A. Zech, I. Y. Zhang, X. Zhang, Y. Zhang, D. Zuev, A. Aspuru-Guzik, A. T. Bell, N. A. Besley, K. B. Bravaya, B. R. Brooks, D. Casanova, J.-D. Chai, S. Coriani, C. J. Cramer, G. Cserey, A. E. DePrinceIII, R. A. DiStasioJr., A. Dreuw, B. D. Dunietz, T. R. Furlani, W. A. GoddardIII, S. Hammes-Schiffer, T. Head-Gordon, W. J. Hehre, C.-P. Hsu, T.-C. Jagau, Y. Jung, A. Klamt, J. Kong, D. S. Lambrecht, W.-Z. Liang, N. J. Mayhall, C. W. McCurdy, J. B. Neaton, C. Ochsenfeld, J. A. Parkhill, R. Peverati, V. A. Rassolov, Y. Shao, L. V. Slipchenko, T. Stauch, R. P. Steele, J. E. Subotnik, A. J. W. Thom, A. Tkatchenko, D. G. Truhlar, T. V. Voorhis, T. A. Wesolowski, K. B. Whaley, H. L. WoodcockIII, P. M. Zimmerman, S. Faraji, P. M. W. Gill, M. Head-Gordon, J. M. Herbert, A. I. Krylov, *J. Chem. Phys.* **2021**, *155*, 84801.

[7] A. Dreuw, M. Head-Gordon, *Chem. Rev.* **2005**, *105*, 4009.

[8] N. Tanaka, T. Kasai, *Bull. Chem. Soc. Jpn.* **1981**, *54*, 3020.

[9] M. Tesmer, H. Vahrenkamp, *Eur. J. Inorg. Chem.* **2001**, 1183.

[10] J. P. Nietfeld, R. L. Schwiderski, T. P. Gonnella, S. C. Rasmussen, *J. Org. Chem.* **2011**, *76*, 6383.

[11] X. Geng, J. T. Mague, J. P. Donahue, R. A. Pascal, *J. Org. Chem.* **2016**, *81*, 3838.